Discrete gene sets depend on POU domain transcription factor Brn3b/Brn-3.2/POU4f2 for their expression in the mouse embryonic retina

Xiuqian Mu[1], Phillip D. Beremand[2], Sheng Zhao[3], Rashmi Pershad[4], Hongxia Sun[1], Ann Scarpa[1], Shuguang Liang[1], Terry L. Thomas[2] and William H. Klein[1,*]

[1]Department of Biochemistry and Molecular Biology, The University of Texas M. D. Anderson Cancer Center, Houston, TX 77030, USA
[2]Department of Biology and The Laboratory for Functional Genomics, Texas A&M University, College Station, TX 77843-3285, USA
[3]Department of Biomathematics, The University of Texas M. D. Anderson Cancer Center, Houston, TX 77030, USA
[4]Department of Molecular Genetics, The University of Texas M. D. Anderson Cancer Center, Houston, TX 77030, USA
*Author for correspondence (e-mail: wklein@mdanderson.org)

Accepted 27 November 2003

Development 131, 1197-1210
Published by The Company of Biologists 2004
doi:10.1242/dev.01010

Summary

Brn3b/Brn-3.2/POU4f2 is a POU domain transcription factor that is essential for retinal ganglion cell (RGC) differentiation, axonal outgrowth and survival. Our goal was to establish a link between Brn3b and the downstream events leading to RGC differentiation. We sought to determine both the number and types of genes that depend on Brn3b for their expression. RNA probes from wild-type and *Brn3b*$^{-/-}$ E14.5, E16.5 and E18.5 mouse retinas were hybridized to a microarray containing 18,816 retina-expressed cDNAs. At E14.5, we identified 87 genes whose expression was significantly altered in the absence of Brn3b and verified the results by real-time PCR and in situ hybridization. These genes fell into discrete sets that encoded transcription factors, proteins associated with neuron integrity and function, and secreted signaling molecules. We found that Brn3b influenced gene expression in non RGCs of the retina by controlling the expression of secreted signaling molecules such as sonic hedgehog and myostatin/Gdf8. At later developmental stages, additional alterations in gene expression were secondary consequences of aberrant RGC differentiation caused by the absence of Brn3b. Our results demonstrate that a small but crucial fraction of the RGC transcriptome is dependent on Brn3b. The Brn3b-dependent gene sets therefore provide a unique molecular signature for the developing retina.

Supplementary data available online

Key words: POU domain transcription factor, Brn3b/Brn-3.2/POU4f2, Mouse embryonic retina, Microarray gene expression profiling

Introduction

During embryonic development, emerging cell types often rely on key cell-type specific transcription factors, the function of which is to drive events to a differentiated state. Cell-type-specific transcription factors act in combination with other nuclear factors to alter the transcriptional state of the cell. One important group of transcription factors generally associated with the differentiation of neuronal and endocrine cell types is the POU domain-containing proteins. POU domain transcription factors are required for the differentiation of various neuronal cell types in the brain, and in somatosensory, vestibular/cochlear and visual systems (McEvilly and Rosenfeld, 1999; Xiang et al., 1997). The importance of POU domain proteins in neuronal differentiation has been firmly established by phenotypic analysis of gain- and loss-of-function mutants, and by molecular characterization of their DNA-binding and transcriptional activation/repression properties (McEvilly and Rosenfeld, 1999; Wegner et al., 1993). In addition, a number of downstream target genes have been identified that depend on POU domain transcription factors for their normal neuronal expression.

Despite this wealth of information, fundamental questions concerning POU domain proteins and their roles in neuronal differentiation have not been answered. To date there is no clear understanding of the position of individual POU domain factors in the gene regulatory network operating within any differentiating neuronal cell type. Although in some cases particular upstream and downstream genes have been identified (Bermingham et al., 2002; Erkman et al., 2000; Mu et al., 2001; Wagner et al., 2002), we have yet to achieve a clear picture of how POU domain proteins alter the transcriptional states of neuronal cells. We do not even know the number of genes in a particular neuronal cell type that depend on an individual POU factor for their expression. Because the transcriptome of any neuronal cell type consists of thousands of expressed genes, POU domain factors could be associated with a wide spectrum of gene expression involving many different functional gene classes. Alternatively, POU factors could act in more subtle

fashions, causing changes only in a limited number of functional gene classes, leaving most of the transcriptome unaltered.

We have made use of the retinal ganglion cell (RGC)-specific POU domain transcription factor Brn3b/Brn-3.2/POU4f2 to address issues of POU domain protein function in neuronal cells. In the mouse, *Brn3b* (*Pou4f2* – Mouse Genome Informatics) is first expressed at E11.5 in newly forming RGCs that have recently exited the cell cycle, and although not required for the initial specification of RGCs, Brn3b is essential for normal RGC differentiation, axonal outgrowth and survival (Erkman et al., 1996; Erkman et al., 2000; Gan et al., 1999; Gan et al., 1996; Wang et al., 2000). Two related Brn3 factors, Brn3a and Brn3c, also play roles in RGC differentiation (Wang et al., 2002a) (S. W. Wang, unpublished), although only *Brn3b*-knockout mice produce a detectable RGC phenotype. Thus, Brn3b can be used to identify sets of genes that depend on a POU domain transcription factor for their expression.

Several genes whose expression in the retina is affected by the absence of Brn3b have been previously identified (Erkman et al., 2000; Mu et al., 2001), but given the limited scope of these reports, these genes are unlikely to represent the full spectrum of Brn3b function. We previously described the construction of a large database of retina ESTs from E14.5 retinas and a pilot microarray analysis using 864 cDNAs to screen for gene expression alterations in *Brn3b*$^{-/-}$ retinas (Mu et al., 2001). We continue to expand our database, which currently contains over 27,000 retina-expressed cDNAs representing ~15,000 distinct genes (http://odin.mdacc.tmc.edu/RetinalExpress). We estimate that the RetinalExpress database currently contains 60-70% of the genes expressed in the E14.5 retina (Mu et al., 2001).

The embryonic retina represents a tiny proportion of all the tissues that form during the life of a mouse. We have argued that retinal genes highly restricted in their expression will generally be underrepresented in public databases and on commercially available mouse microarrays (Mu et al., 2001). For example, we have identified numerous genes that are present in the RetinalExpress database but not in the 15K NIA or 61K RIKEN mouse EST databases (Mu et al., 2001). Thus, RetinalExpress provides a suitable platform to generate high-density microarrays for use in identifying Brn3b-dependent genes. Below, we describe the identification of Brn3b-dependent genes by comparing expression profiles of wild-type and *Brn3b*$^{-/-}$ retinas using microarrays containing 18,816 retina-expressed cDNAs. We find that highly restricted sets of functional gene classes depend on Brn3b for their expression, including genes that are expressed in non RGCs within the retina. Our results demonstrate that Brn3b controls a small but crucial fraction of the E14.5 retinal transcriptome.

Materials and methods

RNA isolation and aRNA amplification from wild-type and *Brn3b*$^{-/-}$ mice

Wild-type and *Brn3b*$^{-/-}$ mice were maintained in a BL6/129 mixed background. The *Brn3b*$^{-/-}$ allele used in this study was the *Brn3b*$^{GFP\text{-}KI}$ allele described elsewhere (Wang et al., 2002a). Wild-type or *Brn3b*$^{-/-}$ embryos were obtained from pregnant females euthanized after timed mating. Retinas from different embryonic stages were dissected, and total RNA was isolated as described previously Mu et al. (Mu et al., 2001). Total RNA was amplified by the Eberwine method (Van Gelder et al., 1990) using the MassageAmp aRNA kit (Ambion) following the manufacturer's instructions. One microgram of total retinal RNA was used for each amplification, and typically, 50-100 μg of aRNA was obtained after one round of amplification.

Fabrication and processing of retina-expressed cDNA microarray slides

cDNA clones were obtained from the sequenced E14.5 retinal cDNA library. Information on these clones can be found in the RetinalExpress database (http://odin.mdacc.tmc.edu/RetinalExpress). Gene identity of the clones was based mostly on Blastx search results. cDNA inserts from individual clones were amplified in 96-well plates using the T3 and T7 primers as described (Mu et al., 2001). The amplified inserts were purified semi-automatically with the MultiScreen PCR purification system (Millipore) on a Biomek 2000 robotic workstation. To each sample, 20×SSC was added to a final concentration of 3×. The microarrays were printed on PL-100C poly-L-lysine glass slides (CEL Associates) with the OmniGrid microarrayer (Genemachine). A total of 18,816 clones were printed on two slides, and each clone was printed in duplicate. The microarray slides were processed by rehydration and snap-heating, followed by incubation at 80°C for 1.5 hours to crosslink the DNA to the slide surface. The DNA on the slides was then denatured in a 95°C water bath for 2 minutes, rinsed with ethanol and air dried.

Probe labeling and microarray hybridization

aRNA was labeled by direct incorporation of Cy3- or Cy5-dUTP (Amersham) through reverse transcription by SSII (Invitrogen) with 2 or 4 μg of aRNA and 6 μg random primers (Invitrogen) in 30 μl of RT reaction mix (500 μM concentrations of dCTP, dATP and dGTP; 100 μM dTTP, 100 μM Cy3-dUTP or Cy5-dUTP; 400 U SSII; 1 mM DTT; and 1×RT buffer) at 37°C for 2 hours. The RT reactions were terminated, and RNA degraded by addition of 1.5 μl of 0.5 N NaOH and 1.5 μl of 20 mM EDTA (pH 8.0) and heating at 70°C for 10 minutes, followed by addition of 1.5 μl of 0.5 N HCl for neutralization. The Cy3- and Cy5-labeled probes were purified by GFX columns (Amersham Pharmacia) according to the manufacturer's manual, air dried in a SpeedVac, and resuspended in 15 μl of microarray hybridization buffer (see below) and combined.

Microarray hybridization basically followed the TIGR protocol (Hegde et al., 2000) with minor modifications. The slides were first incubated in pre-hybridization buffer (5×SSC, 0.1% SDS and 1% BSA) at 42°C for 1 hour, followed by sequential rinsing in milliQ water and isopropanol and air dried. The 30 μl Cy3- and Cy5-probe mix in 1×hybridization buffer [50% formamide, 5×SSC, 0.1% SDS, 10 μg poly d(A) (Pharmacia) and 10 μg mouse Cot 1 DNA (Invitrogen)] was applied to the microarray slide and covered with HybriSlips (PGC Scientific). Hybridization reactions were carried out in Corning hybridization chambers in a water bath at 42°C overnight. The slides were then washed as follows: 1×SSC, 0.2% SDS at 42°C for 10 minutes; 0.1×SSC, 0.2% SDS at room temperature for 10 minutes; and 0.1×SSC at room temperature for 4 minutes. The slides were air dried and scanned with a GenPix 4000A scanner (Axon) with PMT settings of 500 to 650.

Microarray data collection and analysis

For each hybridized slide, two 16-bit TIFF images representing the Cy3 and Cy5 channels were obtained. The median values of Cy3 and Cy5 signals for individual spots were than obtained with GenPix Pro 4.0 from the TIFF images. The raw data were Lowess normalized (Quackenbush, 2002) and further analyzed with Genespring 5.0 (Silicon Genetics). For normalization, a Lowess curve was fit to the log-intensity versus log-ratio plot. Twenty percent of the data were used to calculate the Lowess fit at each point. This curve was used to adjust the control value for each measurement. If the control channel was lower than 10, then 10 was used instead. Significance of

differentially expressed genes was analyzed by Student's *t*-test with Genespring 5.1.

To compare gene expression changes between different developmental stages, genes with significant changes in all stages (E14.5, E16.5 and E18.5) were combined and the average values for replicate experiments were used to create a clustering gene tree using GeneSpring 5.1 based on similarity of gene expression patterns, which was determined by using the standard correlation and program defaults for separation ratio and minimum distance.

Real-time PCR and data analysis

Real-time PCR was performed on an iCycler (BioRad). Four micrograms of total RNA was first reverse transcribed with SSII and oligo dT primer in a total volume of 20 μl for 2 hours at 42°C. SSII was inactivated by heating at 75°C for 15 minutes, The cDNA was diluted 10 fold, and 1-5 μl was used for each 50 μl PCR using the iQ SYBR Green Supermix (BioRad). The primer sequences can be found in the supplemental data (see Table S1 at http://dev.biologists.org/supplemental. The PCR conditions for all genes were as follows: preheating, 95°C for 3 minutes; cycling, 40 cycles of 94°C for 30 seconds and 50°C for 30 seconds; and 72°C for 40 seconds. For each gene, the real-time PCR assay was performed twice with two different batches of total RNA. The β-actin gene served as an RNA input control.

Fold changes of gene expression were calculated based on the cycle differences between wild-type and *Brn3b*$^{-/-}$ samples as compared to the β-actin control using the following formula: $FC=2^{\Delta MT-\Delta WT}$, where FC is fold change, ΔMT is the difference of cutoff cycles between the gene of interest and the control gene (*β-actin*) for the *Brn3b*$^{-/-}$ and ΔWT is that for wild type.

In situ hybridization

Purified PCR products containing T3 and T7 primer sequences (see above) for genes of interest were used as templates, and DIG-labeled antisense RNA probes were made by in vitro transcription with T7 RNA polymerase (Ambion) and purified by ethanol precipitation. Heterozygous and *Brn3b*$^{-/-}$ embryos were collected at E14.5, fixed with 4% paraformaldehyde, paraffin-embedded, and sectioned at 6 μm. The sections were de-waxed and treated with proteinase K. For each gene, sections from littermates with different genotypes were used, and hybridization was performed side by side. Efforts were made to use sections from similar section planes for individual genes. Hybridization incubations were carried out in hybridization buffer [50% formamide, 5×SSC (pH 4.5-5.0), 1% SDS, 50 μg /ml yeast tRNA, 50 μg/ml heparin] at 65°C overnight, followed by three 30-minute washes with pre-warmed washing buffer [50% formamide, 1×SSC (pH 4.5-5.0), 1% SDS] at 65°C. The slides were then incubated with alkaline phosphatase-conjugated anti-DIG antibody (Roche) in 1×MABT (100 mM maleic acid, 150 mM NaCl, 0.1% Tween 20, pH 7.5), 2% BRB (Roche) and 10% goat serum overnight at room temperature. After being washed five times (30 minutes each) with MABT buffer and once with NTMT [100 mM Tris-HCl (pH 9.5), 100 mM NaCl, 50 mM $MgCl_2$, 0.1% Tween 20 and 0.048% levamisole], hybridization signals were visualized by incubating with BM Purple (Roche) at room temperature for the desired time. The slides were then counterstained with eosin and photographed.

Electrophoretic mobility shift assay

EMSA with GST-3bPOU was performed as described (Gruber et al., 1997). For supershift, 1 μl of anti-GST antibody (Promega) was added to the binding reaction. The sequences for the SBRN3 probe were: 5′ GCACACGACCCAATGAATTAATAACCGGGCTG 3′ and 5′ GCAGCCCGGTTATTAATTCATTGGGTCGTGTG 3′. The Brn3 consensus competitor oligonucleotide sequences were: 5′ GATCT-CTCCTGCATAATTAATTACCCCCGGAT 3′ and 5′ GATCCGG-GGGTAATTAATTATGCAGGAGAGAT 3′.

Cell culture, cell transfection and luciferase assay

HEK 293 cells were cultured in DMEM with 10% FBS at 37°C with 5% CO_2. To generate the luciferase reporter construct, the conserved *sonic hedgehog* region in the first intron was amplified by PCR from mouse genomic DNA and inserted upstream of the minimal rat prolactin promoter (–36prl) driving firefly luciferase expression (Trieu et al., 1999). A mutant version of this *Shh* reporter construct was made by PCR, mutating all the essential nucleotides in the Brn3b-binding site from ATGAATTAAT to GCGCGTTGAC. The Brn3b expression construct was made by placing the *Brn3b* cDNA under the control of the CMV promoter. Transfection was carried out in six-well plates using FuGene (Roche) following the manufacturer's protocol. For each transfection, 10 ng of reporter plasmid, 1 μg of Brn3b expression plasmid or empty vector, and 1 ng of pRL-CMV (Promega) expressing *Renilla* luciferase was used. Cells were harvested 36 hours after transfection, and luciferase activity was measured by the Dual-Luciferase Reporter Assay System (Promega). The firefly luciferase activity was normalized to *Renilla* luciferase activity.

Results

Identification of Brn3b-dependent retina-expressed genes at E14.5

We chose E14.5 as the most crucial developmental time to compare expression profiles from wild-type and *Brn3b*$^{-/-}$ retinas for two reasons. First, at E14.5 RGC differentiation is at its peak, while other cell types have either just begun to differentiate or have not yet begun. Thus, at E14.5, most cells in the retina are either newly formed RGCs within the ganglion cell layer or neuroblasts in various states of commitment in the proliferation zone above the ganglion cell layer. Second, at E14.5, although mutant RGCs are abnormal in appearance and behavior, the number of differentiated RGCs is the same in *Brn3b*-null retinas as it is in wild-type controls (Gan et al., 1999; Wang et al., 2000). At later times, *Brn3b*$^{-/-}$ RGCs undergo enhanced apoptosis, and by P0, the number of RGCs in mutant retinas is 70% less than controls (Gan et al., 1999; Wang et al., 2000). Using RNA from E14.5 thus maximizes the chances of identifying Brn3b-dependent genes while avoiding potential secondary effects from the loss of RGCs observed in later stage mutant retinas.

Three pairs of wild-type and *Brn3b*$^{-/-}$ antisense RNA (aRNA) samples amplified from independent retinal total RNA preparations were labeled by reverse transcription with Cy3 or Cy5 dyes; duplicate experiments were performed for each pair either by exchanging the labeling dye (two pairs) or varying the amount of probe (one pair). In total, six different experiments were performed with replicate microarrays containing 18,816 retina-expressed cDNAs. In all cases, greater than 90% of the spotted cDNAs yielded signals above background. In rare occurrences, dye exchange led to significant differences between wild-type and *Brn3b*$^{-/-}$ signals but these were discounted. After Lowess normalization with Genespring 5.0, the ratio of wild-type to mutant signal was obtained for each cDNA spot in all six experiments. cDNA clones with ratios or inverse ratios of 1.7 or higher in at least four experiments were considered to represent significant changes in expression as measured by Student's *t*-test (Table 1). We chose 1.7-fold change as our empirical cut-off because smaller cut-off values greatly increase the number of false-positive clones.

The analysis produced 157 cDNAs that met the above-

Table 1. Known genes whose expression changes in the absence of Brn3b

Accesssion Number*	Gene name	FC†	FC (PCR)‡	*p*-value§	SE¶
Transcription factors					
S69351	Brn3b/Brn-3.2/Pou4f2	–5.06	–	0.000	RGC
L12147	Olf-1/EBF1	–4.27	–8.0	0.000	RGC
S69350	Brn3a/Brn-3.0/Pou4f1	–3.82	–4.6	0.000	RGC
AF295369	Irx2	–3.81	–5.7	0.000	RGC
AB025922	Gli1	–2.99	–6.1	0.000	Progenitor
AB015132	Ubiquitous Kruppel like factor	–1.87	ND	0.000	Unknown
U51000	Dlx-1	2.18	4.0	0.002	Progenitor
NM_009380	Thyroid T3 hormone receptor beta	2.91	ND	0.001	Non-RGC
NM_010054	Dlx-2	NA	2.8		Progenitor
Neuron integrity and function					
AF099986	Persyn/synuclein-γ	–13.60	–42.2	0.000	RGC
S59158	EAAT-2/GluT1	–3.83	–6.9	0.000	Non-RGC
NM_013031**	VMAT-2	–3.00	–16.0	0.000	RGC
J02809	GAP-43	–2.99	–2.1	0.000	RGC
U10355	Synaptotagmin 4	–2.73	–6.9	0.000	RGC
AF148511	Hermes	–2.53	–4.9	0.000	RGC
M20480	Neurofilament light chain	–2.48	–3.7	0.000	RGC
AF091342	Nerurofilament medium chain	–2.41	–2.6	0.000	RGC
U62325	FE65-like protein	–2.35	ND	0.000	Unknown
M16465	Calpactin I light chain	–2.30	–5.3	0.000	Unknown
AB048947	Synaptotagmin 13	–2.30	ND	0.000	RGC
U59230	Nel-like 2 (nell2)	–2.19	–16.0	0.000	Unknown
D50086	Neuropilin 1	–1.96	–2.6	0.000	Unknown
M18776	Tau microtubule binding protein	–1.83	–2.4	0.000	RGC
AY043013††	Neuron navigator 1 (NAV1)	1.95	ND	0.002	Unknown
Signaling and cell cycle					
X76290	Sonic hedgehog	NA	–78.8		RGC
AF033855	Myostatin/GDF8	–2.05	–12.1	0.000	RGC
AB010833	Ptc2	NA	–4.9		Progenitor
S78355	Cyclin D1	–2.50	–2.4	0.000	Progenitor
Others					
D45913	Leucine-rich-repeat protein	–2.46	ND	0.000	Unknown
AF292939	Glucocorticoid induced gene 1, Gig1	–2.33	–2.0	0.000	Unknown
AP001748	U2 snRNP auxiliary factor	–2.25	ND	0.000	Unknown
BC001993	Protein phosphatase 4	–2.18	ND	0.000	Unknown
BC017139	RIKEN 2310067G05 gene	–2.15	ND	0.000	Unknown
NM_145377	Tripartite motif-containing 41	–2.12	ND	0.000	Unknown
XM_196206	RIKEN 2610209L21 gene	–2.11	ND	0.000	Unknown
AF012271	Visual pigment-like receptor	–2.10	ND	0.000	Unknown
AJ414378	Putative methionyl aminopeptidase	–2.00	ND	0.000	Unknown
D13635††	Ubiquitin-protein isopeptide ligase E3	–1.98	ND	0.000	Unknown
XM_128169	RIKEN 1810041L15 gene (RGCG1)	–1.91	–2.6	0.000	RGC
AB051466	KIAA1679 protein	–1.87	ND	0.000	Unknown
U17259	p19	–1.86	ND	0.001	Unknown
U17599	Ribonucleoprotein	–1.80	–2.6	0.000	Unknown
Y15924	Cystinosin	–1.76	ND	0.000	Unknown
AH009472	Phosphofructokinase 1 C isozyme	–1.71	ND	0.001	Unknown
M17300	Cholesterol-regulated protein C	–1.70	ND	0.000	Unknown
AE003460	MTMR6	1.63	ND	0.002	Unknown
Z49204	NADP transhydrogenase	1.85	1.9	0.001	Unknown
BC006058	RIKEN 2510049I19 gene	1.92	ND	0.001	Unknown
NM_025940	RIKEN 2610042L04 gene	2.52	2.3	0.001	Unknown

*GenBank Accession Number. Rat (**) or human (††) Accession Numbers are shown for genes without a mouse entry in GenBank.

†Average fold change from microarray experiments. Negative numbers mean reduction in expression in the absence of Brn3b and positive numbers mean increase in expression.

‡Fold change determined by real-time PCR. ND, not determined.

§*P* value (Student's *t*-test) based on the microarray data. The value is presented as 0.000 when it is less than 0.0005.

¶Spatial expression pattern.

mentioned criteria, with expression ratios ranging from 1.7 to 13.6, but because some genes were represented by multiple clones, this number fell to 87 distinct cDNAs. One of these was *Brn3b*, which validated the usefulness of the hybridization procedure. Of the remaining 86 cDNAs, 63 were underexpressed in *Brn3b*$^{-/-}$ RNA and 23 were overexpressed. The cDNAs were distributed into 48 known genes and 38 unknown ESTs. The known genes included not only genes whose functions have been well studied, but also those whose full-length cDNA sequence is known but whose function is not (Table 1). The unknown genes represented uncharacterized sequences that were found only in public EST databases or in the mouse genome sequence. A few of these cDNAs probably represented 3′ UTRs of known genes that have no

representation in other databases, but most of them were likely to represent novel cDNAs that have not been identified previously, as they were not near known genes in the mouse genome (data not shown). Because we wished to determine whether Brn3b-dependent genes belonged to specific functional classes, we mainly focused our analysis on genes that had already been characterized. In any event, the results from the microarray analysis were surprising because they revealed that only a small proportion of the expressed genes in the E14.5 retina depended on Brn3b for their expression.

The replicate experiments were highly reproducible with only minor variation from one experiment to the next. This suggested that most of the genes represented on the microarray and dependent on Brn3b for their normal levels of expression were identified in the analysis. In addition, because the cDNAs spotted on the microarray represented ~50% of all E14.5 retina-expressed genes, we expect that additional Brn3b-dependent genes will be identified when more cDNAs are added to the microarray. In fact, we identified three genes not present on the existing microarrays based on their relationships to genes found in the present analysis (Table 1, see below).

A subset of genes showing 1.7 fold or greater differences in expression levels between wild type and *Brn3b*$^{-/-}$ retinas were subjected to real-time PCR analysis. Real-time PCR plots for 14 representative examples are displayed in Fig. 1, and fold changes for 28 genes are summarized in Table 1. The ratios ranged from >80-fold underexpressed in the case of *sonic hedgehog* (*Shh*) to fourfold overexpressed in the case of *Dlx1*. In general, the fold changes observed by real-time PCR tended to be larger than those from the microarray experiments, probably because of the limited dynamic range of the microarray hybridization (Livesey et al., 2000).

Discrete functional sets of Brn3b-dependent genes

Brn3b-dependent genes listed in Table 1 include genes that were previously reported to have altered expression in *Brn3b*$^{-/-}$ retinas including *Gap43* (Mu et al., 2001), *Olf1/Ebf1* (Erkman et al., 2000) and *Brn3a* (Wang et al., 2002a). All three genes were significantly downregulated in the absence of Brn3b. The cellular functions of these genes provided initial clues for explaining the defects observed in *Brn3b*-null RGCs and unraveling the role of Brn3b in RGC differentiation. As we discuss below, transcription factors and proteins associated with neuron integrity and function represent major classes of Brn3b-dependent genes.

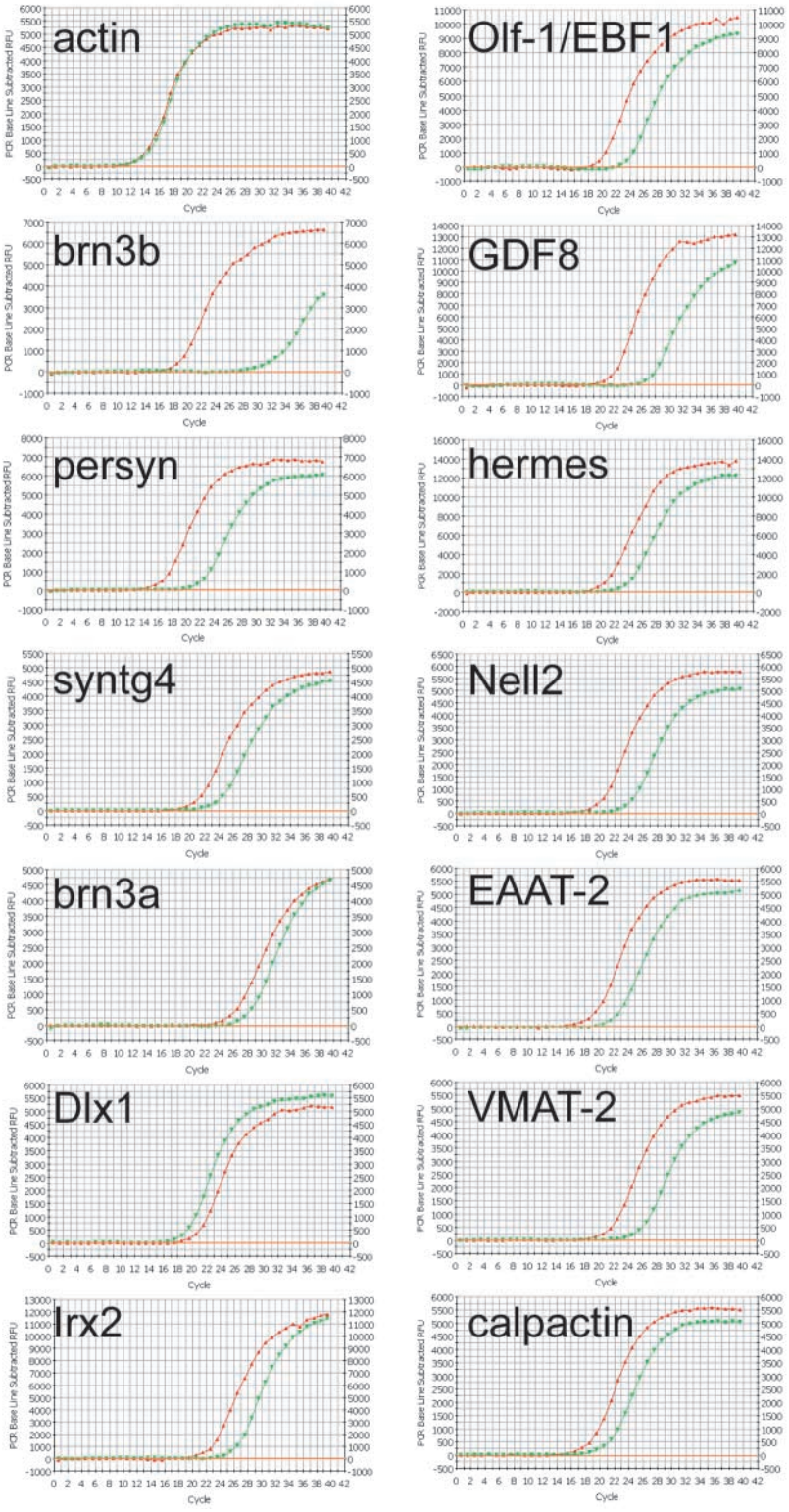

Fig. 1. Real-time PCR confirming the expression changes of subsets of genes in *Brn3b*$^{-/-}$ retina. The *x*-axis is relative fluorescence units (RFU), indicating PCR product accumulation, and the *y*-axis indicates PCR cycles. Wild type is red and *Brn3b*$^{-/-}$ is green. β-actin serves as an RNA input control. Syntg4 is synaptotagmin 4. The accumulation of fluorescence for *Brn3b* in the *Brn3b*$^{-/-}$ sample near the end of the reaction is due to nonspecific amplification, as confirmed by the melting curve and agarose gel electrophoresis (data not shown). Fold changes obtained by real-time PCR are shown in Table 1.

Brn3b-dependent genes encoding transcription factors

Genes encoding transcription factors that were identified in the microarray analysis as underexpressed in *Brn3b*$^{-/-}$ retinal RNA were *Olf1/Ebf1*, *Brn3a*, *Irx2*, *Gli1* and ubiquitous Krupple-like factor. Transcription factor genes that were overexpressed were *Dlx1*, *Dlx2*, and thyroid receptor-β (*TR-β*). With the exception of the gene encoding ubiquitous Krupple-like factor, about which very little is known, the identified genes all have known or postulated roles in the retina.

Olf-1/Ebf1 belongs to a bHLH transcription factor family that also includes Olf2/Ebf2 and Olf-3/Ebf3. The genes encoding these factors are expressed in many post-mitotic neurons during development, including RGCs, suggesting they have a role in neuronal differentiation (Dubois and Vincent, 2001). However, elucidation of their function has been hindered by the potential overlap of the three genes (Dubois and Vincent, 2001).

Brn3a is likely to be a direct target of Brn3b because *brn3a* expression in RGCs immediately follows that of *Brn3b* and the *Brn3a* promoter has Brn3 DNA-binding sites that can stimulate reporter gene transcription when co-transfected into tissue culture cells with Brn3b (Trieu et al., 1999). Although *Brn3a*$^{-/-}$ retinas appear to be normal, *Brn3a-Brn3b* double knockout mice exhibit a more severe RGC phenotype than do *Brn3b*$^{-/-}$ mice, suggesting that Brn3a partially compensates for the loss of Brn3b (S. W. Wang, unpublished).

Irx2 is one of six members of a mammalian homeobox family related to the *Drosophila* genes of the *iroquois* complex. Another member, *Irx6*, which was not included in our array set, has been previously identified as a Brn3b-dependent gene (Erkman et al., 2000). All six Irx genes are expressed in RGCs during development, but their roles in RGC differentiation are unclear (Cohen et al., 2000; Mummenhoff et al., 2001). A recent report suggests that Irx4 is involved in RGC axon pathfinding within the retina through regulating *Slit1* expression (Jin et al., 2003). Not all Irx genes depend on Brn3b for their expression in RGCs; we observed no alterations in expression of *Irx5*, a cDNA that was represented on the retinal cDNA microarray.

Dlx1 and its closely linked relative *Dlx2* are homologs of the *Drosophila* homeobox gene *distal-less*, and they function to downregulate the Notch signaling pathway in neuronal specification and differentiation of the telencephalon (Yun et al., 2002). The strong upregulation of *Dlx1* in the absence of Brn3b prompted us to examine the expression of *Dlx2*, which is linked to *Dlx1* and may be co-regulated with *Dlx1* through common cis-regulatory elements (Panganiban and Rubenstein, 2002). Like *Dlx1*, we found that *Dlx2* was also overexpressed in *Brn3b*$^{-/-}$ RNA (Table 1; Fig. 1). The Notch pathway is crucial for patterning the vertebrate retina and negatively regulating RGC formation (Austin et al., 1995; Dorsky et al., 1995). It is possible that Brn3b is involved in controlling RGC number by negatively regulating *Dlx1* and *Dlx2*. If this were true, *Dlx1* and *Dlx2* expression should be upregulated in *Brn3b*$^{-/-}$ RGCs at E14.5. In situ hybridization of sections from *Brn3b*$^{+/-}$ and *Brn3b*$^{-/-}$ E14.5 embryos showed that *Dlx1* expression was much higher in *Brn3b*$^{-/-}$ retinas than in *Brn3b*$^{+/-}$ retinas (Fig. 2B), supporting the view that Brn3b negatively controls *Dlx1* expression. Notably, *Dlx1* expression was higher in progenitor cells as well as RGCs (Fig. 2B), suggesting that the action of Brn3b might be indirect (see below).

TR-β is a member of the nuclear receptor family, and one of its isoforms TR-β2 is required for the specification of S-cone cells in the photoreceptor layer (Ng et al., 2001). Because *Brn3b* is expressed exclusively in RGCs of the retina, its effects on *TR-β* were unexpected and must be indirect. Although we cannot yet provide an explanation for the upregulation of *TR-β* in the absence of Brn3b, it is possible that Brn3b influences *TR-β* expression in S-cone cell progenitors by regulating genes encoding secreted molecules as discussed below.

Brn3b-dependent genes encoding proteins associated with neuron integrity and function

Consistent with the axonal defects of *Brn3b*$^{-/-}$ RGCs, a battery of neuron-specific cytoskeletal/structural genes were downregulated in *Brn3b*$^{-/-}$ retinas (Table 1; Fig. 2C). The genes encode neurofilament light chain (Nfl), neurofilament middle chain (Nfm), Tau and persyn. Nfl and Nfm are embryonically expressed proteins that form neurofilaments with the postnatally expressed neurofilament heavy chain (Nfh) (Julien, 1999). Tau is a neuron-specific microtubule-associated protein (Garcia and Cleveland, 2001). Persyn (also known as synuclein-γ) belongs to the synuclein family and its gene had the most pronounced reduction in expression in the microarray analysis with a ratio of wild-type to mutant expression of 13.6 (Table 1; Fig. 1, Fig. 3C). The other two members of the family, synuclein-α and synuclein-β, are presynaptic proteins that have been implicated in synaptic function and Alzheimer's disease (Lavedan, 1998), whereas persyn is localized throughout the cell and appears to associate with neurofilament proteins. Overexpression of persyn disturbs the integrity of the neurofilament network (Buchman et al., 1998).

Knockout mice have been generated for several of the above-mentioned genes, but none produced observable neuronal defects, despite being crucial cytoskeletal or structural elements in neuronal cells (Garcia and Cleveland, 2001; Julien, 1999; Ninkina et al., 2003). Compensatory mechanisms, which are largely due to redundancy of related gene family members, are likely to explain the lack of axonal or other neuronal phenotypes. Nevertheless, in the absence of Brn3b, the concerted reduction in expression of several distinct structural components likely contributed to the axonal defects observed in *Brn3b*$^{-/-}$ retinas.

Only a subset of neuron-specific cytoskeletal/structural proteins were identified by our analysis despite the presence of many other neuron-specific genes represented on the microarray. For example, the gene encoding neurofilament 66 (Nf66, also known as α-internexin) is expressed specifically in RGCs of the retina (Levavasseur et al., 1999), but *Nf66* expression levels were unaffected by the absence of Brn3b (Fig. 2A). Because *Nf66* expression served as a marker for the presence of RGCs, comparable levels of *Nf66* transcripts in *Brn3b* heterozygous and homozygous mutant E14.5 retinas further confirmed that, at this developmental time, RGC number was not significantly reduced in *Brn3b*$^{-/-}$ retinas compared with heterozygous controls (Fig. 2A).

In addition to genes encoding neuron-specific cytoskeletal/structural proteins, two genes encoding proteins associated with axon guidance were found to be dependent on Brn3b for their normal expression: neuropilin 1 and Gap43 (Table 1; Fig.

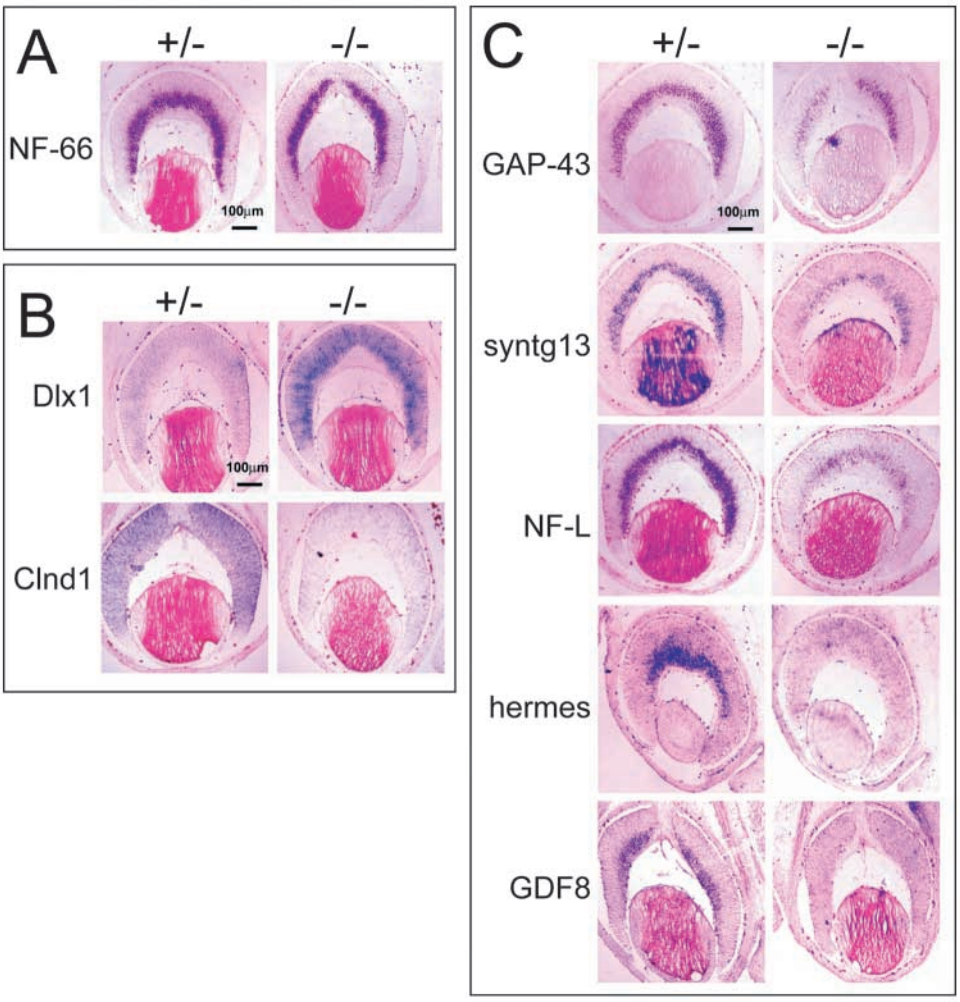

Fig. 2. In situ hybridization for subsets of genes reveals that these genes depend on Brn3b for expression in the retina through both cell-autonomous and non-cell-autonomous mechanisms. DIG-labeled probes for individual genes were hybridized to E14.5 *Brn3b* heterozygous (+/–) and null (–/–) sections across the eye. (A) Consistent with the microarray results, expression of the RGC-specific neurofilament 66 gene (Nf66) was not dependent on Brn3b. (B) Two examples, *Dlx1* and cyclin D1 (Clnd1), whose expression did not coincide with *Brn3b* but was affected by the absence of Brn3b. In the heterozygous retina, both *Dlx*1 and cyclin D1 were expressed mostly in the progenitor cell layer. In the *Brn3b*$^{-/-}$ retina, *Dlx1* was upregulated, most prominently in the RGCs, while cyclin D1 was downregulated. (C) Five examples RGC-specific genes downregulated in the absence of Brn3b: *Gap43*, synaptotagmin 13 (*Syt13*), neurofilament light-chain gene (*Nfl*), Hermes and myostatin/*Gdf8*.

1, Fig. 2C). Although our retina-expressed cDNA microarray included genes for several classes of axon guidance ligands and their receptors, only the genes encoding neuropilin 1 and Gap43 were significantly downregulated in *Brn3b*$^{-/-}$ retinas. Neuropilin 1 complexes with plexins to serve as receptors for class III semaphorins (He et al., 2002). Neuropilin 1 has been implicated in RGC axon guidance at both the optic disc and optic chiasm in *Xenopus* (Campbell et al., 2001). Gap43 also functions in RGC axons at the optic chiasm. Downregulation of the two axon guidance genes is consistent with the pathfinding defects observed in *Brn3b*-null RGC axons (Erkman et al., 2000; Wang et al., 2002a).

Axon guidance and the establishment of the axonal cytoskeletal network are two inseparable aspects of axon growth during neuron development. Growing axons respond to guidance cues by remodeling the cytoskeleton at growth cones (Grunwald and Klein, 2002). Our results suggest that Brn3b plays a central role in both aspects of RGC axon growth by regulating the expression of a subset of the critical genes.

Expression of *Brn3b* persists in RGCs throughout adult life, suggesting that it might also function to regulate genes involved in RGC physiologic integrity. This idea was supported by the identification of several Brn3b-dependent genes involved in physiological processes. These include genes encoding two neurotransmitter proteins Eaat2/Glut1 and Vmat2 (Table 1; Fig. 1). Eaat2/Glut1 is a Na^+/K^+-dependent glutamate transporter belonging to the plasma membrane neurotransmitter transporter family, and Vamt2 is a vesicular monoamine transporter of the vesicular neurotransmitter transporter family (Masson et al., 1999). Both play important roles in synaptic signal transduction.

Three other genes that depended on Brn3b for their normal expression appear to be associated with RGC function. These genes encode synaptotagmin 4, synaptotagmin 13 and calpactin (Table 1; Fig. 1, Fig. 2C). Most members of the synaptotagmin family are calcium sensors for neurotransmitter release at synapses (O'Connor and Lee, 2002). However, synaptotagmin 13 lacks the key amino acid residues required to bind Ca^{2+} ion (von Poser and Sudhof, 2001), while synaptotagmin 4 is mostly localized within the cell body and growth cones, suggesting that this protein may have nonsynaptic functions, perhaps in neurite growth (Ibata et al., 2002). Calpactin forms complexes with many proteins at the plasma membrane. Calpactin is a subunit of annexin II, which functions in neurite growth (Hamre et al., 1995), and it is also an auxiliary protein that associates with two different ion channels (Girard et al., 2002; Okuse et al., 2002). Calpactin thus appears to have both differentiation and physiological functions.

We identified several Brn3b-dependent genes whose

expression was not restricted to neuronal cells but nonetheless were likely to participate in retinal function. Cyclin D1, the only cell cycle gene to be identified in the microarray analysis, was significantly downregulated in the absence of Brn3b (Table 1; Fig. 1, Fig. 2B). Cyclin D1, which promotes progression through the G_1 phase of the cell cycle, is abundantly expressed in the E14.5 retina, and is required in the retina for cell proliferation and photoreceptor cell survival (Dyer and Cepko, 2001; Ma et al., 1998). Cyclin D1 was expressed mostly in progenitor cells in *Brn3b* heterozygous retinas at E14.5 and its expression was uniformly reduced in *Brn3b*-null retinas (Fig. 2B). This result suggests that Brn3b can influence progenitor cell proliferation through cyclin D1. As with *Dlx1* and *Gli1* (see below), the influence of Brn3b on cyclin D1 expression in non RGCs must be indirect.

Hermes is an RNA-binding protein that is strongly downregulated in the absence of Brn3b (Table 1; Fig. 1, Fig. 2C). It is expressed in the developing heart and in RGCs of the retina, but its function is currently not known (Gerber et al., 1999). In RGCs, it may participate in the localization of mRNAs whose encoded proteins are required for normal neurite growth and function.

We also identified a number of uncharacterized genes whose normal expression levels depend on Brn3b (Table 1). Although the roles that these genes play in the retina have not yet been elucidated, some of them would be expected to be RGC-specific and have novel retinal functions. For example, we identified a cDNA, *Rgcg1*, that is identical to the RIKEN mouse cDNA 1810041L15 (Accession Number, XM_205822). The *Rgcg1* gene encodes a predicted 15.9 kDa protein with no recognizable motifs, but an orthologous *Rgcg1* exists in the human genome. Fig. 3A shows that in wild-type sections, *Rgcg1* was expressed specifically in RGCs within the retina and in the olfactory epithelium. In *Brn3b*$^{-/-}$ sections, expression of *Rgcg1* was largely absent in RGCs but was undisturbed in the olfactory epithelium (Fig. 3A). These results identify a new RGC-specific gene and also demonstrate that Brn3b-dependent genes can be expressed outside the retina by mechanisms independent of Brn3b. Below, we discuss further examples of Brn3b-independent expression.

Brn3b-dependent genes encoding secreted signaling molecules

The microarray analysis unexpectedly revealed that the gene encoding myostatin/Gdf8, a member of the TGF-β superfamily, was significantly underrepresented in *Brn3b*$^{-/-}$ retinal RNA (Table 1). Furthermore, real-time PCR showed that myostatin/Gdf8 transcripts were 12-fold reduced in *Brn3b*$^{-/-}$ RNA (Table 1; Fig. 1). Myostatin/Gdf8 is a potent negative regulator of skeletal muscle differentiation but is also strongly expressed in the CNS (McPherron et al., 1997). Our results suggest that myostatin/Gdf8 may have a function in RGCs. In situ hybridization showed that myostatin/*Gdf8* expression in the retina was confined to RGCs in *Brn3b* heterozygous embryos, and that expression was largely absent in *Brn3b*$^{-/-}$ retinas (Fig. 2C). Based on its role in skeletal muscle, myostatin/Gdf8 could be secreted from RGCs into the extracellular retinal environment and negatively impact the differentiation of retinal cell types by preventing progenitor cells from exiting the cell cycle. Myostatin/Gdf8 might play an analogous role to Gdf11, the close homolog of myostatin/Gdf8, which functions as a negative feedback signal in neuronal progenitors of the olfactory epithelium to inhibit the generation of new neurons (Wu et al., 2003).

Because *Gli1* expression levels were reduced in *Brn3b*$^{-/-}$ retinas (Table 1; Fig. 4A,B), and Gli1 is a known component of the Shh signaling pathway, we used real-time

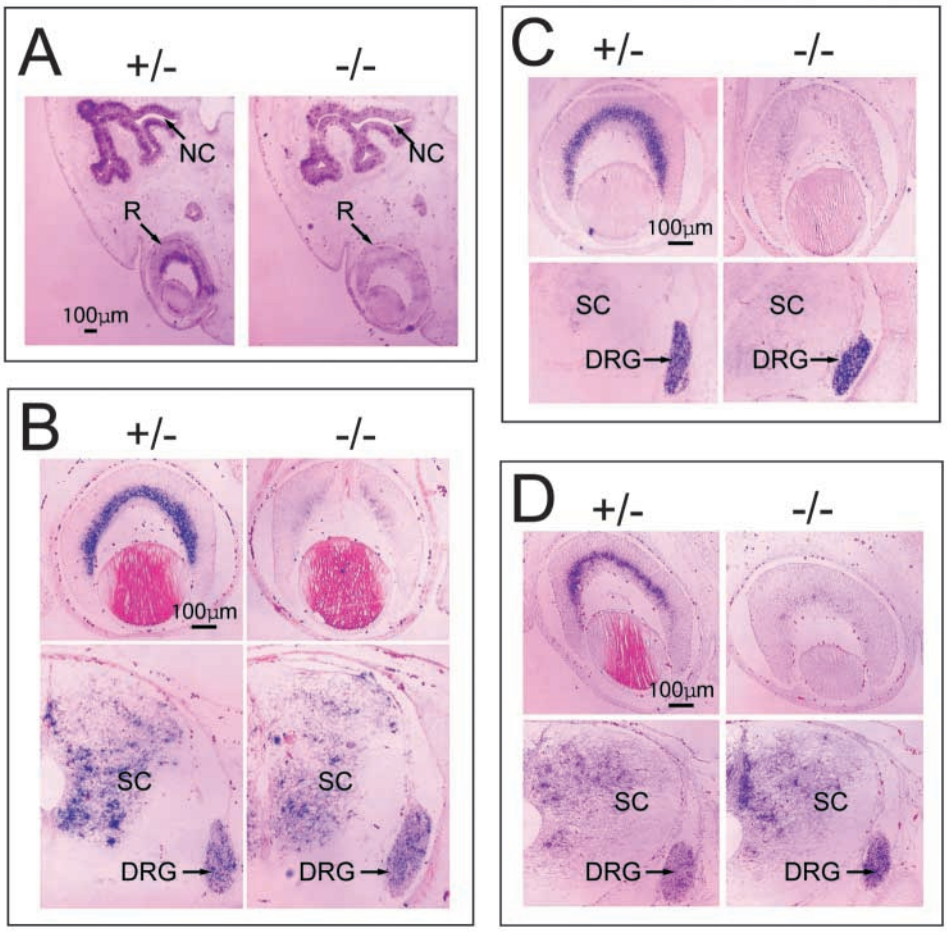

Fig. 3. Brn3b-dependent genes require Brn3b for expression only in the retina. Shown here are four genes (A, *Rgcg1*; B, synaptotagmin 4; C, *persyn*; D, *Brn3a*) whose expression was downregulated in the RGC layer in *Brn3b*-null (–/–) when compared with the heterozygous retina (+/–), but was not changed in other tissues. NC, nasal cavity; R, retina; DRG, dorsal root ganglia; SC, spinal cord.

PCR to determine whether *Shh* expression was altered in the absence of Brn3b. We found that *Shh* levels were reduced about 80-fold in *Brn3b*$^{-/-}$ retinal RNA (Table 1; Fig. 4A). We discuss the significance of this result below but the identification of myostatin/*Gdf8* and *Shh* as Brn3b-dependent genes indicates that Brn3b can exert its function in a cell non-autonomous fashion through the action of secreted signaling molecules.

Genes dependent on Brn3b in RGCs may be expressed independently of Brn3b in non-retinal tissues

Most of the Brn3b-dependent genes that we identified are also expressed outside the retina. Non-retinal expression occurs in tissues both where *Brn3b* is and is not expressed. In both cases, expression of Brn3b-dependent genes was affected only in the retina of *Brn3b*$^{-/-}$ mice. For example, *Brn3a*, persyn and synaptotagmin 4 were expressed in dorsal root ganglia where *Brn3b* is also expressed and in the spinal chord where *Brn3b* is not expressed (Fig. 3B-D). In the absence of Brn3b, expression was reduced in RGCs but unaffected in the dorsal root ganglia and spinal chord (Fig. 3B-D). Similarly, expression of *Rgcg1* was reduced in RGCs of *Brn3b*-mutant embryos but was not reduced in the olfactory epithelium where *Brn3b* is not expressed (Fig. 3A). The results imply that expression of Brn3b-dependent genes is controlled by Brn3b only in the retina and that their expression must be regulated by different mechanisms in other tissues.

The Shh pathway in the retina is controlled by Brn3b

The hedgehog pathway is conserved in most metazoan organisms and is involved in diverse roles in pattern formation and cell differentiation during development (Ingham and McMahon, 2001). In mice, Shh, the major hedgehog factor, binds to its receptors patched 1 (Ptch) or patched 2 (Ptch2), which in turn derepress Smoothend (Smo) to regulate the activity of the effector transcription factors Gli1, Gli2 and Gli3. During retinal development, *Shh* is expressed in RGCs as they commit to their fate (Neumann and Nuesslein-Volhard, 2000; Wang et al., 2002b; Zhang and Yang, 2001a; Zhang and Yang, 2001b). Other members of the pathway, namely, *Ptch*, *Ptch2*, *Smo*, *Gli1*, *Gli2* and *Gli3*, are expressed in retinal progenitor cells (Nakashima et al., 2002) (Fig. 4B). In the retina, *Shh* is required for the autoregulation of RGC number (Zhang and Yang, 2001a) and retinal patterning (Neumann and Nuesslein-Volhard, 2000; Wang et al., 2002b). It has also been shown recently that Shh from RGCs is required for optic disc and stalk neuroepithelial cell development (Dakubo et al., 2003). The observation that *Gli1*, a direct target of Shh signaling, was downregulated in progenitor cells of *Brn3b*$^{-/-}$ retinas (Fig. 4B), suggested that *Shh* expression might also depend on Brn3b.

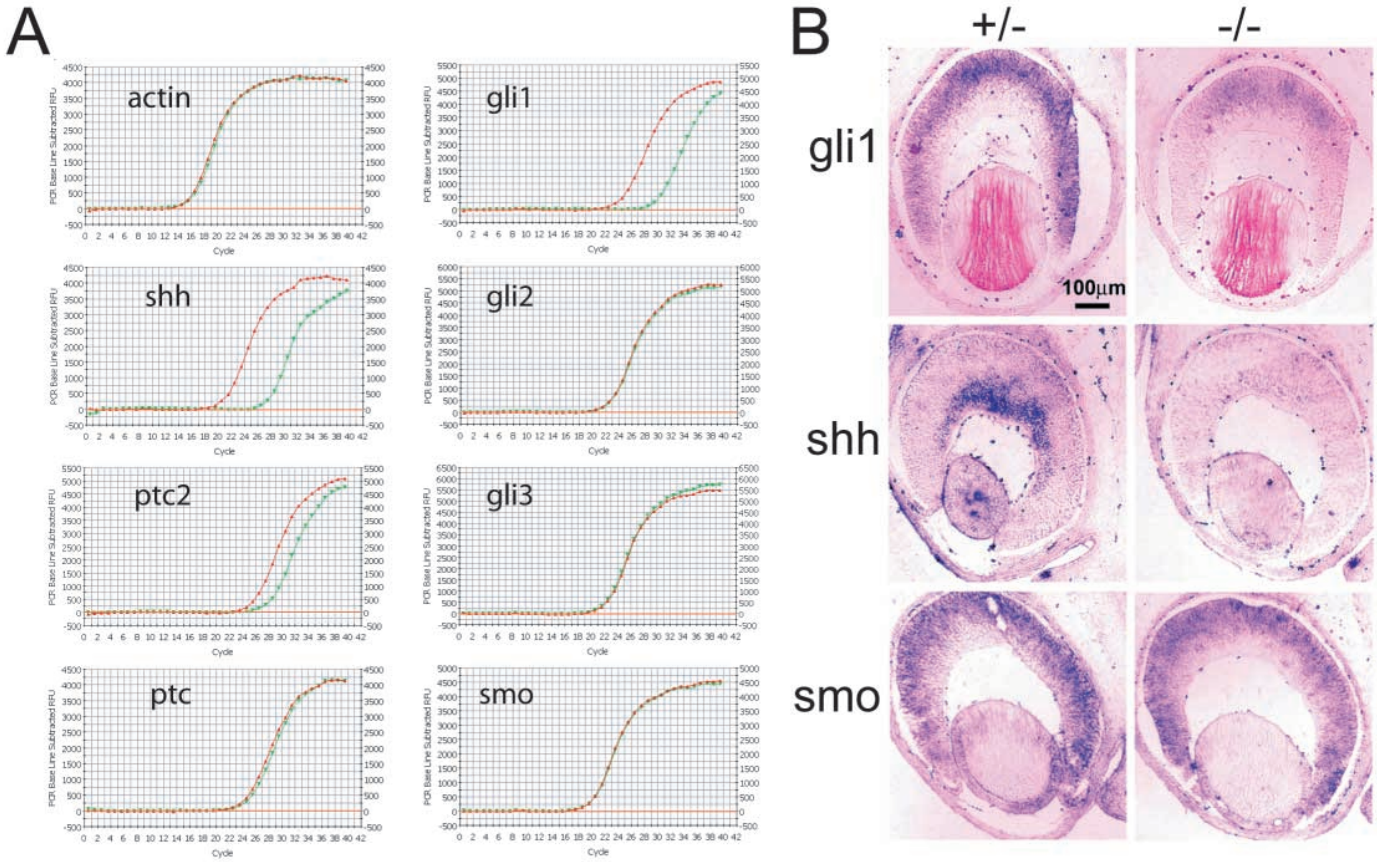

Fig. 4. The sonic hedgehog pathway is disrupted in *Brn3b*$^{-/-}$ retinas. (A) Real-time RT-PCR analysis of genes belonging to the sonic hedgehog pathway. Red is for wild-type and green is for *Brn3b*$^{-/-}$. β-actin was used as RNA input control. Three genes, sonic hedgehog (*Shh*), *Gli1* and patched 2 (*Ptch2*), were significantly downregulated in *Brn3b*$^{-/-}$ retina, while other genes showed no change. (B) In situ hybridization of *Shh*, *Gli1* and *Smo* on E14.5 *Brn3b* heterozygous (+/–) and null (–/–) sections. *Gli1* and *Smo* were expressed in progenitor cells and *Shh* in RGCs. *Gli1* and *Shh* were downregulated in *Brn3b*$^{-/-}$ retinas, while *Smo* showed no change.

This scenario was confirmed by real-time PCR (Fig. 4A) and in situ hybridization (Fig. 4B). As noted above, *Shh* expression in wild-type retina was restricted to RGCs, and this expression was dramatically reduced in *Brn3b*$^{-/-}$ embryos (Fig. 4A,B).

We also examined the dependency of other components of the Shh pathway on Brn3b using real-time PCR. Of those tested, namely, *Ptch*, *Ptch2*, *Gli2*, *Gli3* and *Smo*, only *Ptch2* expression was affected in *Brn3b*$^{-/-}$ retinal RNA. That *Ptch2* expression was altered was consistent with a recent report that loss of Shh signaling mostly affected *Ptch2* expression but not expression of *Ptch* (Wang et al., 2002b). As reported earlier, *Smo* was expressed in progenitor cells in the proliferating zone of the E14.5 wild-type retina and that expression was unaltered in the *Brn3b*$^{-/-}$ retina (Fig. 4B). Taken together, these results suggest that Brn3b controls the Shh pathway in the retina by regulating the expression of *Shh* in RGCs, thereby controlling the expression of downstream target genes like *Gli1* in retinal progenitor cells.

To address whether *Shh* was directly regulated by Brn3b, we searched for Brn3 DNA-binding sites within a region of the *Shh* gene known to contain transcriptional regulatory sequences capable of driving gene expression in the retina (Neumann and Nuesslein-Volhard, 2000). By comparing the *Shh* genomic sequences of four species (mouse, human, zebrafish and Fugu), we found a potential Brn3 DNA-binding site (SBRN3) in a highly conserved 67 bp region in the first intron of *Shh* (Fig. 5A). The Brn3 site was completely conserved in all four species and differed by only one base pair from the previously reported consensus Brn3b DNA-binding sequence (Gruber et al., 1997). To determine whether Brn3b could bind to SBRN3, we performed an electrophoretic mobility shift assay (EMSA) with a GST fusion protein containing the POU domain of Brn3b (GST-3bPOU) and an oligonucleotide probe encompassing SBRN3 (Fig. 5B). GST-3bPOU formed a specific complex with SBRN3, and formation of the complex was inhibited by addition of a competitor Brn3b consensus oligonucleotide or SBRN3 itself, although SBRN3 competition was not as high. The GST-3bPOU-SBRN3 complex was supershifted by an anti-GST antibody (Fig. 5B).

To characterize further the significance of SBRN3 in mediating transcriptional activation by Brn3b, we performed transient co-transfection experiments with HEK 293 cells. We generated a luciferase reporter construct by placing the conserved mouse *Shh* genomic sequence upstream of the minimal rat prolactin promoter. A mutant reporter construct was also made in which the nucleotides crucial for Brn3b binding were changed (Fig. 6). Vectors containing the prolactin promoter alone or three copies of a known Brn3 consensus binding site (b3s1) upstream of the prolactin promoter (Trieu et al., 1999) were used as negative and positive controls, respectively. Fig. 6 shows the normalized luciferase activity when the reporter constructs were co-transfected with either a Brn3b expression plasmid or an empty vector into HEK 239 cells. Brn3b had little effect on the minimal prolactin promoter alone, but significantly (approximately ninefold) activated transcription through the control construct containing three Brn3b-binding sites. As predicted by the EMSA results (Fig. 5), Brn3b activated transcription through the conserved *Shh* fragment (eightfold) as strongly as through the known Brn3 consensus site (Fig. 6). When the Brn3b binding site was mutated, activation by Brn3b was abolished. Although further confirmation is required, these results suggest that Brn3b

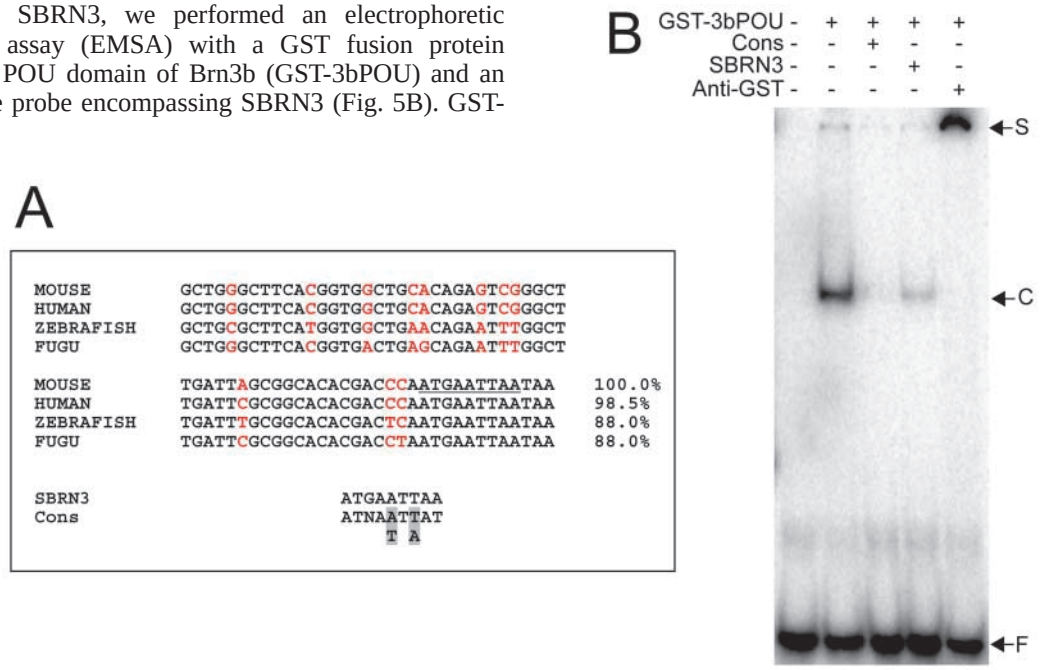

Fig. 5. Brn3b binds to a conserved element (SBRN3) in the *Shh* gene. (A) Alignment of a conserved region in the first intron of *Shh* in mouse, human, zebrafish and Fugu. Red letters indicate nucleotides not conserved among the species. Percentage of identity for each species when compared with the mouse sequence is indicated at the end of the sequences. The Brn3b-binding site (SBRN3) is underlined in the mouse sequence and is completely conserved in all species. The bottom shows the alignment of SBRN3 with the reported consensus Brn3b binding site. (B) Electrophoretic mobility shift assay using a GST-Brn3b POU fusion protein and a ^{32}P-labeled oligonucleotide probe encompassing SBRN3. GST-3bPOU formed a specific complex (C), and formation of this complex was strongly inhibited by both an unlabeled Brn3b consensus oligonucleotide (100×) and the SBRN3 oligonucleotide (100×). A supershifted complex (S) was formed and retained in the loading well when anti-GST antibody was added. F is free SBRN3 probe.

directly regulates *Shh* expression in RGCs, thereby controlling Shh signaling in the retina.

Alterations in gene expression in Brn3b-null retinas at later developmental stages

The results obtained with E14.5 retina provided new insights into the downstream events that depend on Brn3b during RGC differentiation. However, as retina development proceeds, the loss of Brn3b is likely to lead to additional alterations in gene expression. To examine later effects, we isolated wild-type and *Brn3b*-null RNA from E16.5 and E18.5 retinas and performed microarray hybridizations. For each stage, two replicate hybridizations were carried out with two independent pairs of wild-type and *Brn3b*-null RNA pools. Genes with fold changes greater than 1.7 in both duplicate experiments were considered significant.

Genes whose expression was significantly altered at E16.5 and E18.5 were compared with those identified at E14.5, yielding a total of 280 cDNA clones representing 195 non-redundant genes or ESTs (see Table S2 at http://dev.biologists.org/supplemental). Four major clusters (A,B,C and D) emerged from the temporal analysis based on altered expression patterns in the absence of Brn3b (Fig. 7, see Table S2 at http://dev.biologists.org/supplemental). Clusters A and C represented genes that were down- or upregulated, respectively, in the absence of Brn3b at E14.5, i.e. the Brn3b-dependent genes that we described in the previous sections. Alterations in the expression of these genes were likely to be directly related to the loss of Brn3b rather than to secondary (and later) effects of aberrant RGC differentiation. Indeed, many of the E14.5-altered genes were likely to be direct Brn3b targets. Fig. 7 shows that similar alterations in the expression of genes in clusters A and B were observed at E16.5 and E18.5, but overall, the fold change appeared to be less pronounced for most of the genes. We found that many genes in clusters A and C were expressed at lower levels at later developmental stages (data not shown) thus attenuating the fold change in the microarray analysis.

Genes in clusters B and D were not significantly affected at E14.5, but changes in their expression became more pronounced at later stages, with cluster B representing downregulated genes and cluster D representing upregulated ones in the absence of Brn3b (Fig. 7). These genes were not likely to be affected directly by the absence of Brn3b but rather by secondary effects, such as abnormal RGC differentiation and enhanced apoptosis. Most genes in clusters B and D had unknown functions in retina development and many of them had matches only to uncharacterized ESTs in GenBank (see Table S2 at http://dev.biologists.org/supplemental). Nevertheless, most of the ESTs were derived from neural tissues, suggesting a function in neural development.

Genes encoding several transcription factors, including Zn15, Rpf, A-myb (Mybl1 – Mouse Genome Informatics) and Tbx20 were represented in clusters B and D. The late Brn3b dependency on the expression of these genes relative to the much earlier expression of *Brn3b* reveal a complex and dynamic relationship among transcription factors during retina development. However, the biological significance of the late-onset alterations in gene expression in *Brn3b*-null retinas must still be established.

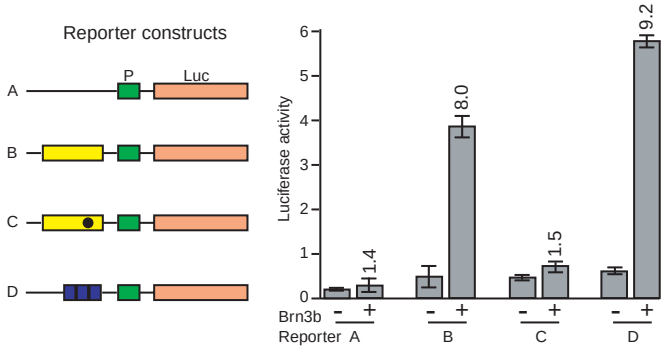

Fig. 6. SBRN3 mediates transcriptional activation by Brn3b in HEK 293 cells. On the left are schematics of the reporter constructs used in the transfection assay. A contains the minimal rat prolactin promoter (–36prl) alone (P, green box) upstream of the luciferase cDNA (Luc); B shows the conserved region (yellow box) in the first intron of mouse *Shh* sequence cloned upstream of –36prl; C is the same as B except that the SBRN3 site is mutated (indicated by a filled black circle); D contains three copies of the consensus Brn3-binding site (blue boxes) upstream of –36prl. On the right is the normalized luciferase activity (in arbitrary units) generated from the reporter constructs co-transfected into HEK 293 cells, with (+) or without (–) the Brn3b expression vector. Each bar represents the average of three replicate experiments. Fold change in luciferase activity for each construct in the presence of Brn3b is indicated at the top of the respective bars.

Discussion

Using microarray technology, we identified discrete sets of genes that depend on the POU domain transcription factor Brn3b for their normal levels of expression in the mouse E14.5 retina. Loss of Brn3b and the subsequent defects in RGC differentiation also caused gene expression alterations at later stages. Genes affected by the loss of Brn3b at E14.5 were more likely to be directly related to the function of Brn3b than genes affected at later times in development. The Brn3b-dependent gene sets at E14.5 are largely, but not entirely, defined by three functional classes: genes encoding transcription factors; genes associated with neuron integrity and function; and genes encoding secreted signaling molecules. In addition, a number of other Brn3b-dependent genes were also identified that were not assigned to these classes, including unknown genes and uncharacterized ESTs. Notably, we found no alterations in the expression of genes encoding apoptotic proteins, even though *Brn3b*$^{-/-}$ RGCs undergo enhanced apoptosis. This suggests that the enhanced apoptosis observed in *Brn3b*-mutant RGCs is secondary to the initial defects in differentiation.

The identification of Brn3b-dependent genes involved in neuron integrity and function is consistent with the differentiation defects observed in *Brn3b*$^{-/-}$ RGCs. However, alterations in the expression of some key genes in *Brn3b*$^{-/-}$ retinas could not be explained when compared with previous reports regarding the function of these genes in retinal development. For example, although cyclin D1 expression was significantly reduced in the absence of Brn3b, no cell proliferation or photoreceptor cell defects were observed in *Brn3b*-null retinas, as has been reported for cyclin D1-mutant retinas (Dyer and Cepko, 2001). Similarly, *Shh* expression was reduced to very low levels in *Brn3b*$^{-/-}$ retinas, but neither RGC

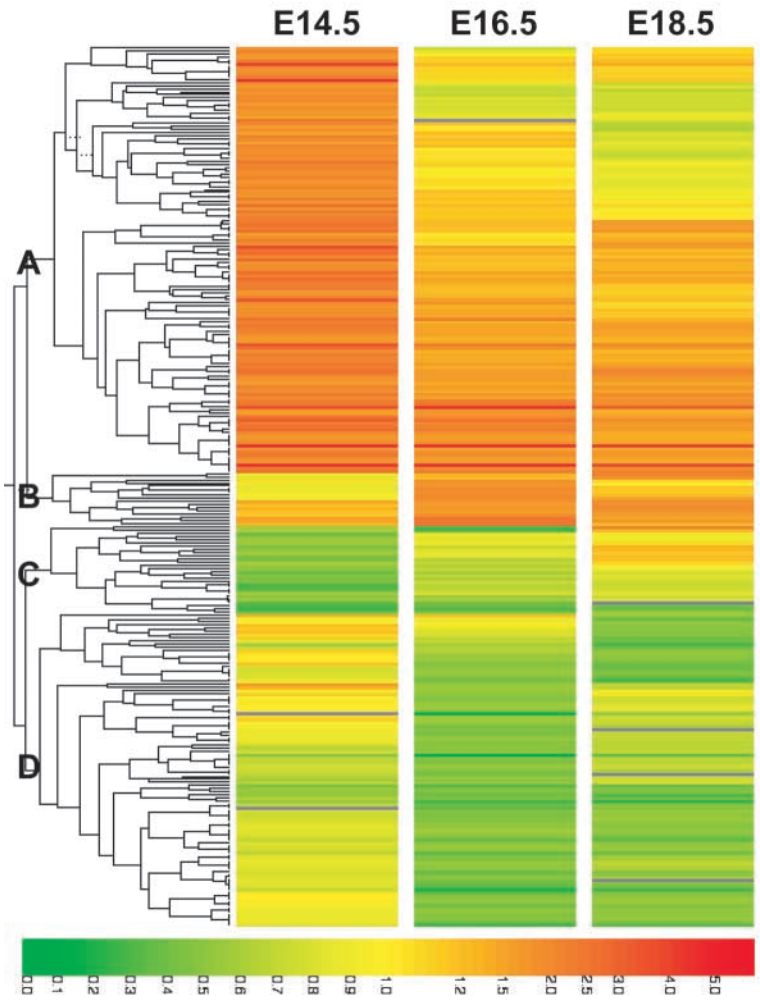

Fig. 7. Alterations in *Brn3b*-dependent gene expression at different stages of retina development. Each column represents one developmental stage (E14.5, E16.5 and E18.5) and each horizontal line represents one cDNA clone. Fold changes (wild type/*Brn3b*-null) are color-coded according to the bar at the bottom of the figure; red represents downregulation in Brn3b-null retina and green represents upregulation. The cDNA clones were clustered according to similarities their expression patterns as shown by the tree of the right side of the figure. The four major clusters, A, B, C and D, are discussed in the text.

overproduction nor retinal disorganization were observed, as would be predicted from *Shh* gain- or loss-of-function studies (Neumann and Nuesslein-Volhard, 2000; Wang et al., 2002b; Zhang and Yang, 2001a; Zhang and Yang, 2001b). One possible explanation is that in the absence of Brn3b, residual expression is sufficient for wild-type activity. Alternatively, Brn3b may regulate molecular events that have opposing biological effects. Brn3b plays a positive role in RGC differentiation but it might also inhibit RGC production through negative-feedback mechanisms involving Shh and myostatin/Gdf8. In addition, loss of Brn3b might result in compensating changes in the expression of genes closely related to genes such as cyclin D1, *Shh* and myostatin/*Gdf8*. The phenotype of *Brn3b*$^{-/-}$ retinas reflects the net effects of the deregulation of all Brn3b-dependent genes, which is not necessarily a simple sum of their phenotypes.

A major conclusion from our study is that retinal expression of only a limited number of genes and functional gene classes was altered in the absence of Brn3b. Eighty-seven genes were identified with alterations in expression at E14.5 from a screen of 18,816 retina-expressed cDNAs, which represented an estimated 12,000 genes (Mu et al., 2001). Given that this number of genes corresponds to roughly 50% of the total E14.5 retinal transcriptome, we predict that no more than ~200 expressed genes in the E14.5 retina will be included in the Brn3b-dependent gene sets.

In general, our analysis did not distinguish between genes that were under the direct control of Brn3b and genes that depended on Brn3b only indirectly, through the action of other transcription factors. Clearly, the genes encoding *Dlx1*, *Gli1* and cyclin D1 were indirectly affected because these genes are not expressed in RGCs, the only retinal cells that express *Brn3b*. Furthermore, many genes that are directly regulated by Brn3b probably have promoter/enhancer elements that use other transcription factors in addition to Brn3b, including those transcription factors identified as Brn3b dependent. The transcriptional activity of Brn3b has not been clearly defined, although it appears that Brn3b is capable of transcriptional activation or repression, depending on the cellular and promoter context (Budhram-Mahadeo et al., 1999; Plaza et al., 1999). When measured by real-time PCR, up- or downregulation of Brn3b-dependent genes ranged from twice the value observed in wild-type RNA to more than 40 times, suggesting that a variety of transcriptional readout mechanisms exist that rely partly or completely on Brn3b. Positive or negative feedback mechanisms involving Brn3b-dependent transcription factors would be interrupted in the absence of Brn3b and this would also affect transcriptional readout. Although tightly defined in terms of number and functional class, the gene regulatory events downstream of Brn3b are likely to be exceedingly complex and interconnected.

Because the expression of several genes encoding transcription factors was significantly affected by the loss of Brn3b and these regulatory factors would further alter the expression of other downstream genes, it might be expected that the gene regulatory network downstream of Brn3b would extend to hundreds to thousands of genes. That this was not the case suggests that transcriptional events independent of Brn3b partially compensate for the alterations in gene expression caused by the absence of Brn3b. In fact, many of the identified Brn3b-dependent genes encoding transcription factors have close relatives that are expressed in the retina but are apparently not under the control of Brn3b, *Irx5* for example. These genes could compensate for the reduction in expression of their Brn3b-dependent relatives. Brn3b clearly represents an important node in the gene regulatory network that leads to RGC differentiation because RGCs cannot differentiate normally without it and most die by P0. By contrast, genes encoding several important classes of transcription factors that are known to be expressed in RGCs are not essential for RGC differentiation as determined by lack of retinal phenotypes in knockout mice. Gene redundancy may explain the lack of

observed RGC phenotypes in many cases, including redundancy in the *Olf/Ebf* and *Irx* gene families (Cohen et al., 2000; Dubois and Vincent, 2001; Mummenhoff et al., 2001). Even for Brn3b, significant redundancy exists because more severe RGC phenotypes are observed in *Brn3a*$^{-/-}$; *Brn3b*$^{-/-}$ and *Brn3b*$^{-/-}$; *Brn3c*$^{-/-}$ double knockout mice than in *Brn3b*$^{-/-}$ single knockout mice (Wang et al., 2002a) (Steven Wang and W.H.K., unpublished). These results suggest that at least some Brn3b-dependent genes will be more dramatically affected in the double knockout retinas because of the partially overlapping functions of Brn3a, Brn3b and Brn3c.

The expression of many RGC-specific genes was unaffected by the loss of Brn3b. Some examples include *Pax6*, *Nf66*, *Snap25*, and *Scg10*. *Pax6*, which is expressed in RGCs at E14.5, has been reported to be a potential target of Brn3b (Plaza et al., 1999). Our results suggest that Brn3b is not essential for *Pax6* expression. The results imply that the expression of these genes must be under the control of RGC transcription factors that function independently of and parallel to Brn3b. Control of RGC differentiation thus appears to be highly robust and adaptable, with both compensatory and parallel pathways at work to complement the action of Brn3b. The Brn3b-dependent gene sets thus represent a highly definable and unique molecular signature for RGCs within the E14.5 retina. We envision that other RGC transcription factors will be defined by their own RGC signatures once they are subjected to similar gene expression profiling analyses. Ultimately, applying this approach to several key transcription factors would provide a detailed picture of the entire RGC gene regulatory network leading from the regulatory genes at the top of the hierarchy to the terminal downstream genes at the bottom that define the differentiated cell type. In this regard, Math5 (Atoh7 – Mouse Genome Informatics), a bHLH transcription factor expressed in retinal progenitor cells and essential for RGC specification, is positioned genetically upstream of Brn3b (Brown et al., 1998; Brown et al., 2001; Wang et al., 2001). Math5-dependent genes should therefore include the Brn3b gene sets defined here, intermediate genes positioned between *Math5* and *Brn3b*, and other genes associated with the *Math5* progenitor cell population.

We thank Mini Kapoor for help in scanning the microarray slides, Randy Johnson for the mouse *Shh* probe, Eric Turner for the GST-Brn3b POU expression construct and prolactin promoter reporter constructs, and Jeff Villinski for helpful discussions and assistance with graphics. We also thank the other members of the Klein Laboratory for discussions and encouragement. This work was supported by NIH-NEI grants EY11930 and EY13523, and by the Robert A. Welch Foundation. The University of Texas M. D. Anderson DNA Sequencing Facility is supported in part by an NIH-NCI Cancer Center Support Grant (CA16672).

References

Austin, C. P., Feldman, D. E., Ida, J. A., Jr and Cepko, C. L. (1995). Vertebrate retinal ganglion cells are selected from competent progenitors by the action of Notch. *Development* **121**, 3637-3650.

Bermingham, J. R., Jr, Shumas, S., Whisenhunt, T., Sirkowski, E. E., O'Connell, S., Scherer, S. S. and Rosenfeld, M. G. (2002). Identification of genes that are downregulated in the absence of the POU domain transcription factor pou3f1 (Oct-6, Tst-1, SCIP) in sciatic nerve. *J. Neurosci.* **22**, 10217-10231.

Brown, N. L., Kanekar, S., Vetter, M. L., Tucker, P. K., Gemza, D. L. and Glaser, T. (1998). Math5 encodes a murine basic helix-loop-helix transcription factor expressed during early stages of retinal neurogenesis. *Development* **125**, 4821-4833.

Brown, N. L., Patel, S., Brzezinski, J. and Glaser, T. (2001). Math5 is required for retinal ganglion cell and optic nerve formation. *Development* **128**, 2497-2508.

Buchman, V. L., Adu, J., Pinon, L. G., Ninkina, N. N. and Davies, A. M. (1998). Persyn, a member of the synuclein family, influences neurofilament network integrity. *Nat. Neurosci.* **1**, 101-103.

Budhram-Mahadeo, V., Ndisang, D., Ward, T., Weber, B. L. and Latchman, D. S. (1999). The Brn-3b POU family transcription factor represses expression of the BRCA-1 anti-oncogene in breast cancer cells. *Oncogene* **18**, 6684-6691.

Campbell, D. S., Regan, A. G., Lopez, J. S., Tannahill, D., Harris, W. A. and Holt, C. E. (2001). Semaphorin 3A elicits stage-dependent collapse, turning, and branching in Xenopus retinal growth cones. *J. Neurosci.* **21**, 8538-8547.

Cohen, D. R., Cheng, C. W., Cheng, S. H. and Hui, C. C. (2000). Expression of two novel mouse Iroquois homeobox genes during neurogenesis. *Mech. Dev.* **91**, 317-321.

Dakubo, G. D., Wang, Y. P., Mazerolle, C., Campsall, K., McMahon, A. P. and Wallace, V. A. (2003). Retinal ganglion cell-derived sonic hedgehog signaling is required for optic disc and stalk neuroepithelial cell development. *Development* **130**, 2967-2980.

Dorsky, R. I., Rapaport, D. H. and Harris, W. A. (1995). Xotch inhibits cell differentiation in the Xenopus retina. *Neuron* **14**, 487-496.

Dubois, L. and Vincent, A. (2001). The COE-Collier/Olf1/EBF-transcription factors: structural conservation and diversity of developmental functions. *Mech. Dev.* **108**, 3-12.

Dyer, M. A. and Cepko, C. L. (2001). Regulating proliferation during retinal development. *Nat. Rev. Neurosci.* **2**, 333-342.

Erkman, L., McEvilly, R. J., Luo, L., Ryan, A. K., Hooshmand, F., O'Connell, S. M., Keithley, E. M., Rapaport, D. H., Ryan, A. F. and Rosenfeld, M. G. (1996). Role of transcription factors Brn-3.1 and Brn-3.2 in auditory and visual system development. *Nature* **381**, 603-606.

Erkman, L., Yates, P. A., McLaughlin, T., McEvilly, R. J., Whisenhunt, T., O'Connell, S. M., Krones, A. I., Kirby, M. A., Rapaport, D. H., Bermingham, J. R. et al. (2000). A POU domain transcription factor-dependent program regulates axon pathfinding in the vertebrate visual system. *Neuron* **28**, 779-792.

Gan, L., Xiang, M., Zhou, L., Wagner, D. S., Klein, W. H. and Nathans, J. (1996). POU domain factor Brn-3b is required for the development of a large set of retinal ganglion cells. *Proc. Natl. Acad. Sci. USA* **93**, 3920-3925.

Gan, L., Wang, S. W., Huang, Z. and Klein, W. H. (1999). POU domain factor Brn-3b is essential for retinal ganglion cell differentiation and survival but not for initial cell fate specification. *Dev. Biol.* **210**, 469-480.

Garcia, M. L. and Cleveland, D. W. (2001). Going new places using an old MAP: tau, microtubules and human neurodegenerative disease. *Curr. Opin. Cell Biol.* **13**, 41-48.

Gerber, W. V., Yatskievych, T. A., Antin, P. B., Correia, K. M., Conlon, R. A. and Krieg, P. A. (1999). The RNA-binding protein gene, hermes, is expressed at high levels in the developing heart. *Mech. Dev.* **80**, 77-86.

Girard, C., Tinel, N., Terrenoire, C., Romey, G., Lazdunski, M. and Borsotto, M. (2002). p11, an annexin II subunit, an auxiliary protein associated with the background K+ channel, TASK-1. *EMBO J.* **21**, 4439-4448.

Gruber, C. A., Rhee, J. M., Gleiberman, A. and Turner, E. E. (1997). POU domain factors of the Brn-3 class recognize functional DNA elements which are distinctive, symmetrical, and highly conserved in evolution. *Mol. Cell Biol.* **17**, 2391-2400.

Grunwald, I. C. and Klein, R. (2002). Axon guidance: receptor complexes and signaling mechanisms. *Curr. Opin. Neurobiol.* **12**, 250-259.

Hamre, K. M., Chepenik, K. P. and Goldowitz, D. (1995). The annexins: specific markers of midline structures and sensory neurons in the developing murine central nervous system. *J. Comp. Neurol.* **352**, 421-435.

He, Z., Wang, K. C., Koprivica, V., Ming, G. and Song, H. J. (2002). Knowing how to navigate: mechanisms of semaphorin signaling in the nervous system. *Sci. STKE*, RE1.

Hegde, P., Qi, R., Abernathy, K., Gay, C., Dharap, S., Gaspard, R., Hughes, J. E., Snesrud, E., Lee, N. and Quackenbush, J. (2000). A concise guide to cDNA microarray analysis. *Biotechniques* **29**, 548-550, 552-554, 556.

Ibata, K., Hashikawa, T., Tsuboi, T., Terakawa, S., Liang, F., Mizutani, A., Fukuda, M. and Mikoshiba, K. (2002). Non-polarized distribution of

synaptotagmin IV in neurons: evidence that synaptotagmin IV is not a synaptic vesicle protein. *Neurosci. Res.* **43**, 401-406.
Ingham, P. W. and McMahon, A. P. (2001). Hedgehog signaling in animal development: paradigms and principles. *Genes Dev.* **15**, 3059-3087.
Jin, Z., Zhang, J., Klar, A., Chedotal, A., Rao, Y., Cepko, C. L. and Bao, Z. Z. (2003). Irx4-mediated regulation of Slit1 expression contributes to the definition of early axonal paths inside the retina. *Development* **130**, 1037-1048.
Julien, J. P. (1999). Neurofilament functions in health and disease. *Curr. Opin. Neurobiol.* **9**, 554-560.
Lavedan, C. (1998). The synuclein family. *Genome Res.* **8**, 871-880.
Levavasseur, F., Zhu, Q. and Julien, J. P. (1999). No requirement of alpha-internexin for nervous system development and for radial growth of axons. *Mol. Brain Res.* **69**, 104-112.
Livesey, F. J., Furukawa, T., Steffen, M. A., Church, G. M. and Cepko, C. L. (2000). Microarray analysis of the transcriptional network controlled by the photoreceptor homeobox gene Crx. *Curr. Biol.* **10**, 301-310.
Ma, C., Papermaster, D. and Cepko, C. L. (1998). A unique pattern of photoreceptor degeneration in cyclin D1 mutant mice. *Proc. Natl. Acad. Sci. USA* **95**, 9938-9943.
Masson, J., Sagne, C., Hamon, M. and El Mestikawy, S. (1999). Neurotransmitter transporters in the central nervous system. *Pharmacol. Rev.* **51**, 439-464.
McEvilly, R. J. and Rosenfeld, M. G. (1999). The role of POU domain proteins in the regulation of mammalian pituitary and nervous system development. *Prog. Nucleic Acid Res. Mol. Biol.* **63**, 223-255.
McPherron, A. C., Lawler, A. M. and Lee, S. J. (1997). Regulation of skeletal muscle mass in mice by a new TGF-beta superfamily member. *Nature* **387**, 83-90.
Mu, X., Zhao, S., Pershad, R., Hsieh, T. F., Scarpa, A., Wang, S. W., White, R. A., Beremand, P. D., Thomas, T. L., Gan, L. et al. (2001). Gene expression in the developing mouse retina by EST sequencing and microarray analysis. *Nucleic Acids Res.* **29**, 4983-4993.
Mummenhoff, J., Houweling, A. C., Peters, T., Christoffels, V. M. and Ruther, U. (2001). Expression of Irx6 during mouse morphogenesis. *Mech. Dev.* **103**, 193-195.
Nakashima, M., Tanese, N., Ito, M., Auerbach, W., Bai, C., Furukawa, T., Toyono, T., Akamine, A. and Joyner, A. L. (2002). A novel gene, GliH1, with homology to the Gli zinc finger domain not required for mouse development. *Mech. Dev.* **119**, 21.
Neumann, C. J. and Nuesslein-Volhard, C. (2000). Patterning of the zebrafish retina by a wave of sonic hedgehog activity. *Science* **289**, 2137-2139.
Ng, L., Hurley, J. B., Dierks, B., Srinivas, M., Salto, C., Vennstrom, B., Reh, T. A. and Forrest, D. (2001). A thyroid hormone receptor that is required for the development of green cone photoreceptors. *Nat. Genet.* **27**, 94-98.
Ninkina, N., Papachroni, K., Robertson, D. C., Schmidt, O., Delaney, L., O'Neill, F., Court, F., Rosenthal, A., Fleetwood-Walker, S. M., Davies, A. M. et al. (2003). Neurons expressing the highest levels of gamma-synuclein are unaffected by targeted inactivation of the gene. *Mol. Cell Biol.* **23**, 8233-8245.
O'Connor, V. and Lee, A. G. (2002). Synaptic vesicle fusion and synaptotagmin: 2B or not 2B? *Nat. Neurosci.* **5**, 823-824.
Okuse, K., Malik-Hall, M., Baker, M. D., Poon, W. Y., Kong, H., Chao, M. V. and Wood, J. N. (2002). Annexin II light chain regulates sensory neuron-specific sodium channel expression. *Nature* **417**, 653-656.
Panganiban, G. and Rubenstein, J. L. (2002). Developmental functions of the Distal-less/Dlx homeobox genes. *Development* **129**, 4371-4386.
Plaza, S., Hennemann, H., Moroy, T., Saule, S. and Dozier, C. (1999). Evidence that POU factor Brn-3B regulates expression of Pax-6 in neuroretina cells. *J. Neurobiol.* **41**, 349-358.
Quackenbush, J. (2002). Microarray data normalization and transformation. *Nat. Genet. Suppl.* 496-501.
Trieu, M., Rhee, J. M., Fedtsova, N. and Turner, E. E. (1999). Autoregulatory sequences are revealed by complex stability screening of the mouse brn-3.0 locus. *J. Neurosci.* **19**, 6549-6558.
Van Gelder, R. N., von Zastrow, M. E., Yool, A., Dement, W. C., Barchas, J. D. and Eberwine, J. H. (1990). Amplified RNA synthesized from limited quantities of heterogeneous cDNA. *Proc. Natl. Acad. Sci. USA* **87**, 1663-1667.
von Poser, C. and Sudhof, T. C. (2001). Synaptotagmin 13: structure and expression of a novel synaptotagmin. *Eur. J. Cell Biol.* **80**, 41-47.
Wagner, N., Wagner, K. D., Schley, G., Coupland, S. E., Heimann, H., Grantyn, R. and Scholz, H. (2002). The Wilms' tumor suppressor Wt1 is associated with the differentiation of retinoblastoma cells. *Cell Growth Differ.* **13**, 297-305.
Wang, S. W., Gan, L., Martin, S. E. and Klein, W. H. (2000). Abnormal polarization and axon outgrowth in retinal ganglion cells lacking the POU-domain transcription factor Brn-3b. *Mol. Cell Neurosci.* **16**, 141-156.
Wang, S. W., Kim, B. S., Ding, K., Wang, H., Sun, D., Johnson, R. L., Klein, W. H. and Gan, L. (2001). Requirement for math5 in the development of retinal ganglion cells. *Genes Dev.* **15**, 24-29.
Wang, S. W., Mu, X., Bowers, W. J., Kim, D. S., Plas, D. J., Crair, M. C., Federoff, H. J., Gan, L. and Klein, W. H. (2002a). Brn3b/Brn3c double knockout mice reveal an unsuspected role for Brn3c in retinal ganglion cell axon outgrowth. *Development* **129**, 467-477.
Wang, Y. P., Dakubo, G., Howley, P., Campsall, K. D., Mazarolle, C. J., Shiga, S. A., Lewis, P. M., McMahon, A. P. and Wallace, V. A. (2002b). Development of normal retinal organization depends on Sonic hedgehog signaling from ganglion cells. *Nat. Neurosci.* **5**, 831-832.
Wegner, M., Drolet, D. W. and Rosenfeld, M. G. (1993). POU-domain proteins: structure and function of developmental regulators. *Curr. Opin. Cell Biol.* **5**, 488-498.
Wu, H. H., Ivkovic, S., Murray, R. C., Jaramillo, S., Lyons, K. M., Johnson, J. E. and Calof, A. L. (2003). Autoregulation of Neurogenesis by GDF11. *Neuron* **37**, 197-207.
Xiang, M., Gan, L., Li, D., Zhou, L., Chen, Z. Y., Wagner, D., O'Malley, B. W., Jr, Klein, W. and Nathans, J. (1997). Role of the Brn-3 family of POU-domain genes in the development of the auditory/vestibular, somatosensory, and visual systems. *Cold Spring Harb. Symp. Quant. Biol.* **62**, 325-336.
Yun, K., Fischman, S., Johnson, J., de Angelis, M. H., Weinmaster, G. and Rubenstein, J. L. (2002). Modulation of the notch signaling by Mash1 and Dlx1/2 regulates sequential specification and differentiation of progenitor cell types in the subcortical telencephalon. *Development* **129**, 5029-5040.
Zhang, X. M. and Yang, X. J. (2001a). Regulation of retinal ganglion cell production by Sonic hedgehog. *Development* **128**, 943-957.
Zhang, X. M. and Yang, X. J. (2001b). Temporal and spatial effects of Sonic hedgehog signaling in chick eye morphogenesis. *Dev. Biol.* **233**, 271-290.

Table S1. Primer sets used for real-time PCR		
Gene	Position	5'-sequence-3'
β-Actin	Forward	CAACGGCTCCGGCATGTGC
	Reverse	CTCTTGCTCTGGGCCTCG
Brn3b	Forward	TCTGGAAGCCTACTTCGCCA
	Reverse	CCGGTTCACAATCTCTCTGA
Brn3a	Forward	AGGCCTATTTTGCCGTACAA
	Reverse	CGTCTCACACCCTCCTCAGT
Gap-43	Forward	GTGCTGCTAAAGCTACCACT
	Reverse	CTTCAGAGTGGAGCTGAGAA
Persyn	Forward	GTACAAAGTGTCACCTCAGT
	Reverse	CAGCAGCATCTGATTGGTGA
Eaat-2/Glut1	Forward	GCTCCCAAATGGTCTAGAGT
	Reverse	GTTGAGATATAGCTCTCCAT
Nfl	Forward	AGCTGAGGAGGCCAAGGAT
	Reverse	CCACTCTGCAAGCAAACAGA
Gli1	Forward	AACTTTCACCGTGGGAGTAA
	Reverse	GGCACTAGAGTTGAGGAATT
Hermes	Forward	CGAAGATGGCCAAGAACAAA
	Reverse	GGCTGTTGTGAAGTCTTGAA
Tau1	Forward	GCAAAGTGACCTCCAAGTGT
	Reverse	CCTGATCACAAACCCTGCTT
Dlx1	Forward	AGAGAGGACCAATGAGCCTT
	Reverse	CACGGTGGATTTCAATCGGT
Calpactin	Forward	CACGCCATGGAAACCATGAT
	Reverse	AAGAAGCAGTGGGGCAGATT
RIKEN 1810041L15 gene (RGCG1)	Forward	TGGGAGGTAAACATGAGAGT
	Reverse	TCCAACCACAGCCATGAAGT
Ribonucleoprotein	Forward	CCCCTGATTCTGATGAGAGT
	Reverse	TTCCTGGTACACCTCAGGAT
Nfm	Forward	AAAGTGGTGGTCACCAAGAA
	Reverse	CAGTTCCCTCATATTGCACA
Cyclin D1	Forward	GCACTTTTGGTCAGCTAGCT
	Reverse	GACATGGCCCTAAACCTTCT
Gig1	Forward	TGTACATAGATGCGTCGAGT
	Reverse	AGGACTACCCAGCAAATCCT
Neuropilin 1	Forward	GAGTAATTACTCAGAGGCGT
	Reverse	AGAAGAATCCACCACAGGGT
Synaptotagmin 13	Forward	CACAGCAAAGGAGCCATCT
	Reverse	GCATCTCCTCCCAGTGGCT
RIKEN 2610042L04 gene	Forward	CATGGCTGTAATGGGCTGTA
	Reverse	AGCAACACTCTCCTTTTGGA
Nell2	Forward	CACAGATGACCTTTCCTGCT
	Reverse	CAGCACAAATGGCCATTCTT
Vmat2	Forward	TGCCAGCGAGCATCTCTTAT
	Reverse	CTTCCTTAGCAGGTGGACTT
Synaptotagmin 4	Forward	TGTTGTAGGTGATGGTTTCA
	Reverse	AGACCATGGTTCTTAGGTGA
Irx2	Forward	GTCCTTCAGAAGTGGAAACA
	Reverse	AGGTATCTCCCTGTTGTACA
Olf1/Ebf1	Forward	CAGCAGTGAAACAGAAGAGT
	Reverse	TCAGTATTTGCAAGGTCGGT
Gli2	Forward	ATGCCTTGGGTTGCTGTGGA
	Reverse	CAACCTTCCGCTCAACCACA
Smoothened	Forward	CAGGCCTCTGAAAGACATGT
	Reverse	GTTCTTGAATGTGGGGCACT
Patched 2	Forward	GCATCAAACTGAGTGCCATC
	Reverse	GTCTGTGGACTCTCCTTGTA
Patched	Forward	CAGACATCAGCCTCCCTTGA
	Reverse	AGAAGCCGTCACAGTGGTGA
Gli3	Forward	ATCCATGGGCACCACCAACA
	Reverse	GACACATCCCAATCAGGTGA
Dlx2	Forward	CTTCATCCATTGCCAGTGGA
	Reverse	AAACATAGGGACTGCTGAGG
Sonic hedgehog	Forward	TGTCATCGAGGAGCACAGCT
	Reverse	AGCTGGACTTGACCGCCATT

Table S2. Non-redundant list of all genes with altered expression in *brn3b*-null retina

Gene ID	Gene name or matched EST	E14.5*	E14.5 *t*-test	E16.5*	E16.5 *t*-test	E18.5*	E18.5 *t*-test
Cluster A							
0251-95	(AF099986) persyn	13.60	0.000	10.79	0.030	4.94	0.001
2092-73	Brn3b	5.06	0.000	1.04	0.754	1.15	0.331
2061-59	EBF/OLF1	4.27	0.000	1.25	0.179	1.45	0.099
2042-68	Genomic Chr 11	3.99	0.000	1.54	0.098	1.62	0.010
2082-14	(S59158) glutamate transporter, GluT-1	3.83	0.000	1.72	0.007	1.29	0.061
4034-04	Irx2	3.81	0.000	4.90	0.000	3.33	0.003
2074-94	Brn3a	3.41	0.000	2.76	0.071	2.10	0.013
2033-50	monoamine transporter Slc18a2	3.00	0.000	1.54	0.051	1.51	0.009
0103-63	(AB025922) Gli1	2.99	0.000	1.26	0.233	1.08	0.560
2082-36	(J02809) calmodulin-binding protein/GAP-43	2.89	0.000	2.36	0.000	1.65	0.025
0822-11	(U10355) synaptotagmin 4	2.73	0.000	1.61	0.018	2.28	0.019
0104-46	No match	2.68	0.000	1.27	0.645	1.32	0.090
2121-19	Genomic	2.66	0.000	1.30	0.322	1.71	0.061
2024-89	Hermes	2.53	0.000	1.66	0.002	1.52	0.084
2084-92	(D45913) leucine-rich-repeat protein	2.46	0.000	1.18	0.222	0.97	0.877
4051-37	(AF031880) light molecular-weight neurofilament	2.46	0.000	2.49	0.017	2.06	0.140
2114-89	Genomic Chr 7	2.42	0.000	1.44	0.032	1.47	0.060
4091-04	Genomic	2.36	0.000	1.08	0.558	1.44	0.317
0223-17	(AB037848) KIAA1427 protein	2.35	0.000	1.93	0.082	1.79	0.010
0181-87	No seq	2.33	0.000	2.11	0.091	1.89	0.099
2021-02	glucocorticoid induced gene 1, Gig1	2.33	0.000	1.08	0.618	1.12	0.502
0054-86	No seq	2.32	0.000	1.48	0.264	1.47	0.014
4094-04	(M16465) calpactin I light chain	2.30	0.000	2.42	0.004	1.87	0.022
2073-83	(AP001748) U2 snRNP auxiliary factor	2.25	0.000	1.03	0.864	0.88	0.398
4011-73	(U62325) FE65-like protein sapiens	2.21	0.000	1.56	0.037	1.61	0.046
3191-54	(X05640) NF-M	2.19	0.000	1.43	0.052	1.42	0.030
4061-63	(BC001993) protein phosphatase 4	2.18	0.000	1.26	0.082	0.84	0.393
2034-93	Cyclin D1	2.16	0.000	1.02	0.918	0.84	0.328
2114-73	Mus musculus RIKEN cDNA 2310067G05 gene	2.15	0.000	1.42	0.048	1.39	0.051
0261-66	No seq	2.14	0.000	1.10	0.457	0.91	0.566
0054-78	No seq	2.14	0.000	0.88	0.540	1.07	0.587
0222-60	Trim41	2.12	0.000	1.28	0.230	1.36	0.338
2114-60	Mus musculus RIKEN cDNA 2610209L21 gene (2610209L21Rik), mRNA Length = 2352	2.11	0.000	1.24	0.154	1.21	0.184
0083-04	(AF012271) visual pigment-like receptor	2.10	0.000	1.10	0.587	1.09	0.572
4041-04	(AF033855) myostatin; growth/differentiation factor 8	2.05	0.000	1.58	0.071	1.84	0.019
4061-62	(AB048947) synaptotagmin XIII	2.05	0.000	1.88	0.001	1.47	0.069
0823-47	No seq	2.05	0.000	1.82	0.049	1.08	0.587
3164-21	No match	2.02	0.000	1.06	0.894	1.09	0.638
2083-44	Genomic Chr 1	2.00	0.000	0.68	0.238	0.77	0.543
2114-82	(AJ414378) putative methionyl aminopeptidase	2.00	0.000	1.87	0.077	1.57	0.028
4041-19	(D13635) KIAA0010 ubiquitin-protein isopeptide ligase (E3)	1.98	0.000	1.57	0.014	1.53	0.016
3223-75	No seq	1.98	0.000	1.05	0.801	0.65	0.250
4012-82	Genomic Chr4, human homologue	1.97	0.000	1.03	0.871	1.36	0.041
2071-68	Genomic Chr4, human homologue	1.97	0.000	1.39	0.022	1.32	0.270
2071-25	(D50086) neuropilin	1.96	0.000	1.25	0.193	1.33	0.127
2121-55	Mus musculus adult male thymus cDNA, RIKEN full-length enriched library, clone: 5830453E13 product: EST, full insert sequence Length = 2695	1.94	0.000	0.96	0.830	0.90	0.552
0253-32	No seq	1.94	0.000	1.04	0.754	1.84	0.072
0242-27	Mus musculus RIKEN cDNA 1810041L15 gene	1.91	0.000	1.22	0.183	0.92	0.591
0191-20	(AB015132) ubiquitous Kruppel like factor	1.87	0.000	1.47	0.054	1.17	0.409
3224-89	(AB051466) KIAA1679 protein	1.87	0.000	1.51	0.059	1.17	0.568
0233-55	(U17259) p19	1.86	0.001	1.50	0.016	1.20	0.506
2084-36	Mus musculus adult male corpora quadrigemina cDNA, RIKEN full-length enriched library, clone: B230380D18 product: EST, full insert sequence Length = 2092	1.84	0.000	1.13	0.428	0.96	0.799
2084-31	No match	1.82	0.000	0.72	0.517	1.08	0.688
0264-76	(U17599) ribonucleoprotein	1.80	0.000	1.66	0.018	1.47	0.008
2042-19	Homologous to Human Chr 10 sequence	1.80	0.000	1.22	0.157	1.33	0.137
3204-67	(M18775) tau microtubule binding protein	1.79	0.000	1.20	0.205	0.97	0.896
2052-01	Genomic	1.78	0.000	1.24	0.227	1.05	0.759
2014-87	(Y15924) cystinosin	1.76	0.000	1.57	0.053	1.43	0.269
0104-38	No match	1.74	0.000	1.30	0.295	1.11	0.678
4062-84	Homologous to human genomic sequence	1.73	0.000	1.39	0.058	1.08	0.568
3174-95	Mus musculus phosphofructokinase-1 C isozyme (Pfkc)	1.71	0.000	0.84	0.550	0.80	0.338
4071-16	No seq	1.70	0.000	1.37	0.041	1.33	0.031
0121-68	(M17300) cholesterol-regulated protein C	1.70	0.000	1.42	0.118	1.45	0.358
3141-43	Mus musculus adult male medulla oblongata cDNA, RIKEN full-length enriched library, clone: 6330582C22	1.70	0.000	0.56	0.094	0.78	0.201
4011-29	Mus musculus adult male hippocampus cDNA, RIKEN full-length enriched library, clone: C630030A18	1.65	0.000	1.15	0.291	0.89	0.507

	product:hypothetical protein						
0251-51	Genomic Chr 1	1.61	0.000	1.02	0.906	0.68	0.270
0272-08	No seq	1.60	0.000	0.86	0.659	0.91	0.673
Cluster B							
3172-45	(AB040905) KIAA1472 protein	1.63	0.001	1.83	0.002	1.41	0.048
4061-70	(X52625) cytosolic 3-hydroxy-3-methylglutaryl coenzyme A synthase	1.58	0.000	1.76	0.020	1.88	0.051
4063-10	Mus musculus RIKEN cDNA D130012K04 gene (D130012K04Rik)	1.52	0.000	2.63	0.013	1.60	0.158
2082-76	(AF179273) alpha-synuclein	1.34	0.000	1.74	0.013	1.99	0.008
4081-39	(AK012551) putative	1.22	0.077	1.64	0.096	1.75	0.003
0612-09	Homo sapiens KIAA1856 protein (KIAA1856),	1.18	0.131	1.91	0.002	1.69	0.021
4051-88	(AJ132046) ZG29p	1.02	0.800	1.95	0.004	1.07	0.871
2034-33	Mus musculus RIKEN cDNA 2600016J21 gene (2600016J21Rik)	0.97	0.796	2.06	0.026	1.31	0.210
2062-75	(U15734) taipoxin-associated calcium binding protein	0.91	0.127	1.94	0.010	1.14	0.463
4093-96	Sumiko/Golga5	0.91	0.298	1.76	0.014	0.98	0.905
4103-42	(BC006185) follistatin-like	0.89	0.230	1.37	0.083	2.13	0.052
4032-88	Mus musculus hypothetical protein C130008N12, mRNA (cDNA clone MGC:54831 IMAGE:6468505), complete cds Length = 3959	0.89	0.179	2.07	0.145	1.62	0.085
4092-89	No seq	0.87	0.076	1.28	0.404	1.96	0.026
0821-29	No seq	0.86	0.036	1.90	0.002	1.26	0.232
Cluster C							
3133-37	Mus musculus 10 days neonate cerebellum cDNA, RIKEN full-length enriched library, clone: B930088P06 product:unclassifiable, full insert sequence Length = 3168	0.66	0.302	0.48	0.277	0.44	0.425
0821-30	No match	0.63	0.004	0.77	0.308	1.05	0.716
0173-30	No match	0.61	0.005	0.67	0.185	0.84	0.336
3224-73	Genomic human homologue	0.61	0.001	0.87	0.327	1.18	0.193
2092-63	Genomic Chr2	0.60	0.021	0.48	0.087	0.50	0.069
0054-77	Mus musculus RIKEN cDNA 5330429B09 gene (5330429B09Rik), mRNA Length = 1195	0.60	0.000	0.82	0.406	0.88	0.506
0104-37	Genomic Chr 6	0.57	0.307	0.61	0.245	0.28	0.149
0192-40	M.musculus TSC-22 mRNA	0.56	0.000	0.87	0.360	0.91	0.612
2083-77	Mus musculus diadenosine triphosphate hydrolase (Fhit) gene, intron 5, partial sequence	0.55	0.029	0.48	0.177	0.48	0.102
2103-14	Mus musculus 3 days neonate thymus cDNA, RIKEN full-length enriched library, clone: A630096G04 product:un classifiable, full insert sequence Length = 3295, has Human homologue	0.55	0.015	0.86	0.373	0.97	0.868
0222-55	Mus musculus 10 days neonate cerebellum cDNA, RIKEN full-length enriched library, clone: B930031I09 product: EST, full insert sequence Length = 2460	0.55	0.002	0.46	0.095	0.76	0.378
2011-80	No match	0.54	0.004	0.86	0.572	1.28	0.192
2122-01	(Z49204) NADP transhydrogenase	0.54	0.000	0.65	0.094	0.95	0.802
2091-37	No seq	0.54	0.077	0.29	0.036	0.23	0.122
0052-01	No seq	0.53	0.146	0.40	0.059	0.31	0.103
4011-88	(BC006058) RIKEN cDNA 2510049I19 gene	0.52	0.000	0.57	0.169	0.75	0.147
0244-37	Mus musculus neuron navigator 1, mRNA (cDNA clone MGC:32500 IMAGE:5055436), complete cds Length = 1992	0.51	0.000	0.72	0.418	0.85	0.542
0081-82	No match	0.47	0.000	0.88	0.625	1.28	0.140
2084-37	(AF134858) espin	0.46	0.048	0.12	0.468	0.35	0.132
2123-87	(U51000) DLX-1	0.46	0.000	0.61	0.161	0.81	0.260
2083-30	No seq	0.43	0.126	0.31	0.260	0.39	0.193
3181-90	No match	0.42	0.001	0.65	0.201	1.20	0.218
0051-02	Mus musculus 9 days embryo whole body cDNA, RIKEN full-length enriched library, clone: D030067A13 product:unclassifiable, full insert sequence Length = 3152	0.41	0.256	0.48	0.199	0.59	0.084
0184-86	Mus musculus RIKEN cDNA 2610042L04 gene (2610042L04Rik), mRNA Length = 1992	0.40	0.000	0.97	0.801	0.93	0.707
2111-40	Mus musculus 12 days embryo embryonic body between diaphragm region and neck cDNA, RIKEN full-length enriched library, clone: 9430039D06 product: EST, full insert sequence Length = 3825	0.38	0.000	0.59	0.129	0.75	0.258
4101-25	(BC004964) oxoglutarate dehydrogenase	0.33	0.525	0.41	0.212	ND	ND
0054-22	Genomic Chr 2	0.31	0.002	0.41	0.096	0.43	0.208
2041-54	TR	0.25	0.001	0.67	0.137	0.73	0.286
Cluster D							
3134-12	No seq	ND	ND	0.36	0.177	0.49	0.509
0193-73	Mus musculus 7 days neonate cerebellum cDNA, RIKEN full-length enriched library, clone: A730028G07	ND	ND	0.10	0.297	0.50	0.177
2112-49	No match	0.9	0.498	0.47	0.072	0.61	0.147
2111-28	Genomic	1.35	0.002	0.57	0.102	0.66	0.131

3132-54	(AF007268) fibroblast growth factor	1.29	0.222	1.18	0.637	0.57	0.107
3132-36	Mus musculus adult male medulla oblongata cDNA, RIKEN full-length enriched library, clone: 6330504A06 product: EST, full insert sequence	1.20	0.062	0.98	0.960	0.53	0.088
2104-16	(S66385) CREB-binding protein, CBP	1.18	0.037	0.82	0.403	0.52	0.087
3132-71	Mus musculus RIKEN cDNA 1110014K08 gene (1110014K08Rik), mRNA Length = 1414	1.16	0.765	0.47	0.071	0.42	0.453
2084-04	Genomic Chr 15	1.12	0.457	0.70	0.219	0.42	0.153
2083-49	(AK022823) unnamed protein product	1.11	0.136	0.66	0.081	0.55	0.061
2093-10	Mus musculus 13 days embryo head cDNA, RIKEN full-length enriched library, clone: 3110023M17 product:hypothetical P-loop containing nucleotide triphosphate hydrolases structure containing protein, full insert sequence	1.09	0.552	0.55	0.072	0.91	0.601
0051-36	Mus musculus RhoB mRNA, complete cds	1.08	0.512	0.57	0.074	0.75	0.197
0111-55	No match	1.07	0.334	0.57	0.092	0.76	0.209
0173-10	No seq	1.05	0.667	0.83	0.628	0.52	0.164
0123-03	(M77842) oculorhombin	1.04	0.590	0.58	0.061	0.54	0.109
0054-28	No match	1.01	0.890	0.43	0.041	0.50	0.117
0053-26	(U91935) retina-derived POU-domain factor	1.01	0.951	0.57	0.086	0.51	0.130
3132-02	(AB029019) KIAA1096 protein	1.01	0.940	0.57	0.064	0.61	0.332
0243-04	Homologous to human genomic sequence	1.01	0.960	0.57	0.093	0.82	0.308
0053-96	Genomic Chr 2	1.01	0.967	0.56	0.175	0.50	0.121
0084-95	(X78443) ribosomal protein L24	1.00	0.979	0.52	0.087	0.77	0.268
0051-91	(D29640) KIAA0051 Ras GTPase-activating-like protein IQGAP1	0.99	0.930	0.47	0.079	0.50	0.132
0051-52	Mus musculus down-regulator of transcription 1 (Dr1),	0.98	0.814	0.54	0.095	0.84	0.294
2111-21	No match	0.98	0.848	0.57	0.081	0.73	0.178
2122-05	Mus musculus RIKEN cDNA 5830406C15 gene (5830406C15Rik)	0.97	0.818	0.49	0.084	0.77	0.278
2092-38	(AF017806) Zn-15 transcription factor	0.97	0.725	0.41	0.137	0.49	0.108
0191-72	(AK001782) unnamed protein product	0.97	0.692	0.57	0.043	0.88	0.410
0102-69	Mus musculus RIKEN cDNA 2210022N24 gene, mRNA	0.97	0.773	0.89	0.705	0.34	0.107
3204-03	(AF044588) protein regulating cytokinesi	0.96	0.749	0.50	0.110	ND	ND
0114-32	No seq	0.95	0.657	0.44	0.062	0.60	0.146
2042-26	(AF017445) GDP-L-fucose pyrophosphorylase	0.95	0.612	0.55	0.062	0.97	0.882
2112-83	(X06656) connexin43 (AA 1-382)	0.94	0.497	0.95	0.771	0.53	0.068
0051-08	Mus musculus RIKEN cDNA 4933426K21 gene (4933426K21Rik), mRNA	0.93	0.484	0.56	0.084	0.75	0.283
0234-22	Mus musculus 10 days neonate cerebellum cDNA, RIKEN full-length enriched library, clone: B930068K11product:NEPRILYSIN-LIKE PEPTIDASE GAMMA homolog, full insert sequence	0.92	0.461	0.50	0.080	0.73	0.205
2084-06	(X07392) ornithine decarboxylase	0.92	0.359	0.54	0.194	0.55	0.119
2092-69	Mus musculus 16 days neonate cerebellum cDNA, RIKEN full-length enriched library, clone: 9630025H1 product: EST, full insert sequence Length = 2438	0.91	0.416	0.50	0.089	0.70	0.185
2083-23	No match	0.91	0.625	0.55	0.167	0.56	0.163
2083-17	(Y00884) 3.4J polypeptide	0.91	0.411	0.49	0.098	0.53	0.092
2083-64	Genomic Chr14	0.91	0.530	0.51	0.095	0.39	0.117
0052-72	Mus musculus 6 days neonate head cDNA, RIKEN full-length enriched library, clone: 5430420F09 product: EST, full insert sequence Length = 1791	0.90	0.524	0.53	0.096	0.53	0.107
0121-92	(AF163665) germ cell-less protein	0.90	0.584	0.74	0.154	0.45	0.083
0084-79	(AF049330) PPAR gamma coactivator	0.89	0.354	0.49	0.075	0.63	0.191
0052-16	Mus musculus adult male small intestine cDNA, RIKEN full-length enriched library, clone: 2010109C11 product: EST, full insert sequence Length = 991	0.89	0.148	0.46	0.075	0.73	0.142
2083-28	No match	0.89	0.430	0.40	0.141	0.28	0.378
0083-42	No match	0.89	0.206	0.58	0.098	0.72	0.178
2092-14	Genomic Chr 4	0.88	0.444	0.44	0.099	0.47	0.125
3142-58	No match	0.87	0.179	0.54	0.056	0.67	0.453
0051-05	(D13643) KIAA0018 protein	0.87	0.532	0.45	0.102	ND	ND
2121-24	No match	0.86	0.123	0.56	0.070	0.62	0.163
2091-29	(AK001486) unnamed protein product	0.86	0.328	0.53	0.172	0.50	0.078
0052-81	Genomic	0.85	0.561	0.42	0.061	0.48	0.061
0051-10	No match	0.85	0.478	0.61	0.090	0.58	0.068
3142-77	(AL080108) hypothetical protein	0.85	0.144	0.54	0.073	0.67	0.125
0051-29	(U64849) contains similarity to Pfam domain	0.85	0.089	0.54	0.103	0.56	0.123
2083-37	No match	0.83	0.489	0.39	0.116	0.46	0.189
0051-25	Mus musculus adult male thymus cDNA, RIKEN full-length enriched library, clone: 5830487K18 product: EST, full insert sequence Length = 1420	0.83	0.546	0.58	0.132	0.49	0.156
0052-55	Homologous to human genomic sequence	0.83	0.390	0.47	0.106	0.53	0.170

0192-14	(AJ010585) PTB-like protein	0.83	0.324	0.54	0.048	0.74	0.277
2083-68	Genomic Chr. 11	0.82	0.189	0.52	0.167	0.43	0.184
2091-03	No seq	0.82	0.393	0.26	0.108	0.31	0.141
0051-83	(L28174) disulfide-like protein	0.81	0.270	0.52	0.134	0.50	0.104
0051-95	Mus musculus natural killer tumor recognition protein (Nktr) gene, exons 6, 7 and 8, and partial cds Length = 2859	0.81	0.310	0.37	0.110	0.48	0.098
0172-63	No match	0.81	0.113	0.51	0.321	0.59	0.266
2091-49	No match	0.80	0.372	0.55	0.221	0.57	0.075
3143-50	Genomic Chr. 2	0.80	0.240	0.56	0.199	0.58	0.406
0051-66	No match	0.80	0.370	0.55	0.056	0.75	0.206
2094-56	No match	0.80	0.106	0.51	0.087	0.46	0.128
2091-63	Genomic Chr. 4	0.80	0.235	0.48	0.070	0.57	0.220
0051-13	(L35261) transcriptional regulatory protein A-myb	0.79	0.430	0.54	0.157	0.46	0.151
2092-68	Mus musculus 15 days embryo head cDNA, RIKEN full-length enriched library, clone: D930012O21 product: EST, full insert sequence Length = 4290	0.79	0.109	0.55	0.149	0.43	0.106
0054-07	Mus musculus 11 days embryo spinal cord cDNA, RIKEN full-length enriched library, clone: G630008A16 product:unclassifiable, full insert sequence Length = 3275	0.79	0.229	0.50	0.088	0.60	0.072
3132-82	Genomic Chr. 2	0.79	0.317	0.54	0.080	0.77	0.215
2083-06	(U88567) secreted frizzled related protein	0.76	0.018	0.65	0.171	0.45	0.061
0082-46	No match	0.76	0.066	0.50	0.096	0.72	0.281
3141-14	Mus musculus 3 days neonate thymus cDNA, RIKEN full-length enriched library, clone: A630032O12 product:unclassifiable, full insert sequence Length = 1359	0.74	0.070	0.49	0.112	0.61	0.163
0051-39	No match	0.74	0.076	0.43	0.083	0.51	0.063
0234-79	(X83569) neuronatin-2	0.73	0.025	0.56	0.077	0.82	0.301
0054-10	Tbx20	0.72	0.040	0.46	0.081	0.57	0.206
0084-44	No seq	0.72	0.010	0.50	0.085	0.70	0.172
3134-91	(BC000805) similar to rat nuclear ubiquitous casein kinase 2	0.72	0.144	0.45	0.137	ND	ND
0121-25	No seq	0.71	0.251	0.43	0.195	0.67	0.438
2084-53	Mus musculus 13 days embryo lung cDNA, RIKEN full-length enriched library, clone: D430047D06 product:inferred: probable transposase mariner 1 {Homo sapiens}, full insert sequence Length = 2532	0.70	0.152	0.38	0.100	0.35	0.177
2052-85	(AB030190) unnamed protein product	0.70	0.226	0.18	0.105	0.24	0.097
2091-21	No seq	0.67	0.193	0.34	0.099	0.38	0.109
0082-30	(AF106702) testis-enriched protein tyrosine phosphatase	0.66	0.044	0.50	0.062	0.69	0.231
0053-23	(AB023155) KIAA0938 protein	0.64	0.001	0.57	0.069	0.76	0.235

*Average wild-type/*brn3b*-null ratios.
Gene ID indicates ID number in the RetinalExpress database (http://odin.mdacc.tmc.edu/RetinalExpress).
No match indicates no sequence match in GenBank.
No seq. indicates no sequence available for the clone.
Genomic indicates only matches to genomic sequences, in GenBank; mouse chromosome location is given where possible.
ND indicates no data.